

Special Issue on Infectious Disease Modeling

This special issue highlights various applied and computational mathematics approaches that offer insight into the spread of infectious diseases, with particular emphasis on COVID-19.

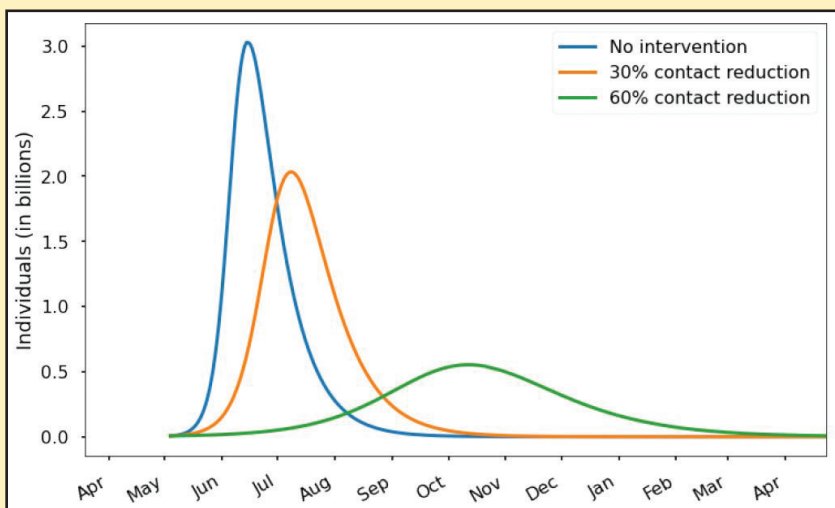


Figure 3. Flattening the curve through contact reduction.

Infectious diseases grow exponentially because each newly-infected person becomes another source of infection. In an article on page 6, David Ketcheson uses an SIR model to study the propagation of COVID-19 in terms of susceptible, infectious, and recovered individuals. He cycles through the model's different stages and accounts for the effect of non-pharmaceutical intervention.

The Forensics of Emerging Diseases

By Matthew R. Francis

New diseases have always been part of humanity's world, but today's highly interconnected global culture facilitates the worldwide spread of epidemics more quickly than ever. To make matters worse, novel zoonotic diseases—brought about by pathogens that jump from animals to humans—pose an ongoing threat because of human practices that bring us into contact with animal species with which we do not generally interact. One such disease is currently running amok across a large part of the world: COVID-19, caused by the previously-unknown severe acute respiratory syndrome coronavirus 2 (SARS-CoV-2).

When a novel infection emerges, researchers face a wide range of challenges, in addition to the obvious medical crises. Two queries are central to these challenges: Where did the disease come from and how bad will it be? Answering these questions requires a combination of detective work, sophisticated mathematics, on-the-ground ecological knowledge, and machine learning.

"It's hard to know what we're preparing for," Michael Johansson, a biologist at the National Center for Emerging and Zoonotic

Infectious Diseases (part of the Centers for Disease Control and Prevention), said. During his talk at the 2020 American Association for the Advancement of Science (AAAS) Annual Meeting, Johansson likened disease forecasting to hurricane prediction. In both cases, deterministic mathematical models—which require constantly-updated data—can only go so far before necessitating supplementation by other methods.

How to Be a Good (Disease) Host

Barbara Han is an ecologist at the Cary Institute of Ecosystem Studies, and her work largely focuses on identification of animal species that harbor novel diseases. During her presentation at the 2020 AAAS Annual Meeting, Han pointed out that most emerging pathogens come from mammals. In fact, over 190 identified unique zoonotic diseases have been associated with mammal species (see Figure 1, on page 4).

"The primary goal is to predict which species would give rise to new zoonotic threats to humans," Han said. "You can look at which rodents, bats, carnivores, and so forth have a high risk of transmitting

See **Emerging Diseases** on page 4

Modelling Global Outbreaks and Proliferation of COVID-19

By Leon Tribe and Robert Smith?

Many of us are experiencing the effects of a pandemic for the first time. We may not be sick, but COVID-19 has disrupted our lives in some manner. From the trivial shortage of toilet paper to massive social and economic upheaval, a microscopic virus is affecting all of us in one way or another. A medical crisis has not impacted the modern world this significantly since the 1918–1919 Spanish influenza pandemic, which was caused by an H1N1 virus.

While advanced models of diseases often employ differential equations to assess virulence, it is clear that the severe acute respiratory syndrome coronavirus 2 (SARS-CoV-2) has two distinct vectors of infection: community transmission and "recent arrivals." The discontinuous nature of recent arrivals introduces multiple sources of infection and complicates analysis. Each new outbreak requires individual study. So, what other techniques

can we apply to achieve a level of certainty in uncertain times?

Determining a Threshold for Action

Although there is growing evidence that a strong national intervention—adopted as early as possible—is key to economic recovery, we can utilize network theory to determine a threshold at which we personally choose to act. If we assume that an individual knows 100 unique people, each of whom has 100 friends, that makes 10,000 people within two degrees of separation from the original person. Therefore, it makes sense to act before the ratio of confirmed cases of a disease reaches a level of 1 per 10,000 within a population.

Why is this so? Because at this level in our idealised network, you know someone who knows someone with the illness. When the density of disease victims exceeds this value, it generates an increased risk of direct exposure to an infected individual. Coincidentally, the threshold of 1 in 10,000

also corresponds to the point at which many countries began to introduce strong measures to combat COVID-19. For example, the day Italy crossed this threshold was the day the country effectively went into lockdown.

Unfortunately, it seems that this threshold is probably too late for adequate national intervention. For instance, Italy saw the density of cases increase to 1 in 1,000, which strained and broke down infrastructure. While beyond the scope of our current analysis, it would be interesting to consider national action before and after this 1 in 10,000 "line in the sand" — or even the 1 in 100,000 threshold as a predictor of rapid recovery.

Predicting the Threshold's Approach

Because a density of 1 in 10,000 provides a theoretical limit as to when effective action can commence at a national and personal level, we may want to predict the threshold's approach. Assuming that

See **Global Outbreaks** on page 3

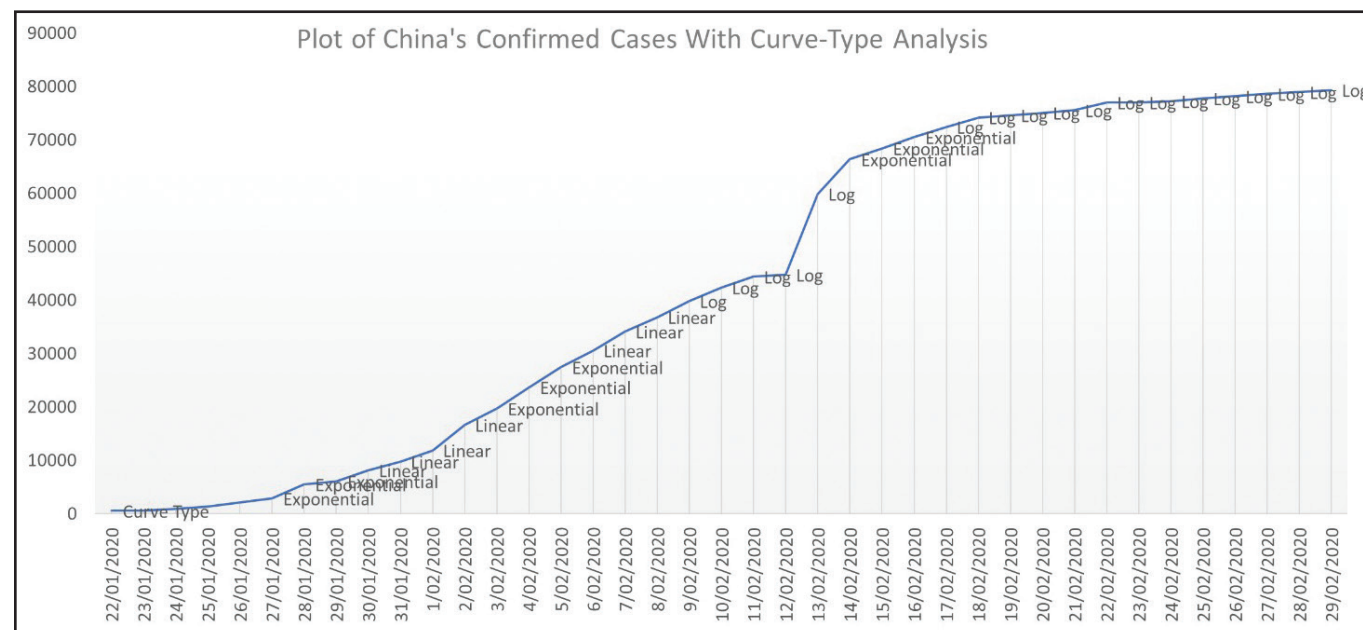


Figure 1. Time course of COVID-19 in China using linear, logarithmic, and exponential best fits. Figure courtesy of Leon Tribe.

Nonprofit Org
U.S. Postage
PAID
Permit No 360
Bellmawr, NJ

siam
SOCIETY for INDUSTRIAL and APPLIED MATHEMATICS
3600 Market Street, 6th Floor
Philadelphia, PA 19104-2688 USA

5 Math and AI-based Repositioning of Existing Drugs for COVID-19

There is presently no specific antiviral drug for the COVID-19 pandemic, which has infected more than two million individuals worldwide. One of the most feasible strategies for treating COVID-19 patients involves drug repositioning, the process of finding new uses for existing drugs. Duc Nguyen and Guo-Wei Wei discuss the mathematical approaches behind the data presentation of structural-based drug repositioning.

6 Looking Ahead to the 2021 SIAM Conference on Computational Science and Engineering

Laura Grigori, Misha Kilmer, and Stefan Wild—co-chairs of the organizing committee for the 2021 SIAM Conference on Computational Science and Engineering (CSE21)—preview what is expected to be SIAM's largest meeting to date. They explore CSE21's central themes and discuss updates that encourage deeper attendee interactions.

8 Seven SIAM Members Elected as AAAS Fellows

In October 2019, the American Association for the Advancement of Science (AAAS) elected seven members of SIAM as 2019 AAAS Fellows in the Section on Mathematics. These individuals were honored for their efforts to advance science and its applications to better serve society at the 2020 AAAS Annual Meeting, which took place this February in Seattle, Wash.



10 A Model to Predict COVID-19 Epidemics with Applications to South Korea, Italy, and Spain

Zhihua Liu, Pierre Magal, Ousmane Seydi, and Glenn Webb present several differential equations models of COVID-19 epidemics that employ early reported case data from around the world to predict the future number of cases. They break the virus down into three phases and apply their models to data from the outbreaks in South Korea, Italy, and Spain.

Message from the Editor-in-chief of SIAM News

By Hans Kaper

All around the world, people are feeling the acute effects of a mass pandemic for what is likely the first time. Employment and education efforts are disrupted, certain resources are in short supply, some hospitals are near capacity, and individuals are practicing social distancing and self-isolation. In response, the May 2020 issue of *SIAM News* highlights some of the tools of applied and computational mathematics that offer insight into the spread of infectious diseases.

This issue is motivated by the worldwide proliferation of the novel severe acute respiratory syndrome coronavirus 2 (SARS-CoV-2) and the current pandemic caused by the associated disease COVID-19, but it addresses other infec-

tious diseases as well. The collection of articles within these pages is certainly not comprehensive, and readers will find that some overlap exists. Our main concern in assembling this compilation was timeliness. Anyone seeking more detailed information should refer to the SIAM Epidemiology Collection, which is freely available to all for one year and accessible online.¹

We thank the authors for their enthusiastic and prompt response to our invitation to contribute to this special issue. Further pieces on the topic of disease modeling and COVID-19 will be published in future issues of *SIAM News*. The suggestion to publish a series of articles on the spread of infectious diseases originated within the

¹ <https://epubs.siam.org/page/EpidemiologyCollection>

SIAM Activity Group on Mathematics of Planet Earth (SIAG/MPE), and we appreciate the SIAG's prompt attention to this timely matter.

As your professional society, SIAM is working hard to help facilitate a better understanding of COVID-19 and the research surrounding it. Please visit snews.siam.org to read additional posts about SIAM's ongoing response to the virus, relevant mathematical resources, funding agency accommodations for travel costs, and more.

Hans Kaper, founding chair of the SIAM Activity Group on Mathematics of Planet Earth and editor-in-chief of SIAM News, is affiliate faculty in the Department of Mathematics and Statistics at Georgetown University.

Choosing Intervention Strategies During an Emerging Epidemic

By Lauren M. Childs

The early weeks and months of 2020 were overshadowed by the rapidly spreading novel severe acute respiratory syndrome coronavirus 2 (SARS-CoV-2) that originated in Wuhan, China, in December 2019. By the beginning of April, the coronavirus disease (COVID-19) epidemic had reached nearly every country in the world, with well over a million cases and more than 50,000 deaths [3]. Because the epidemic's spread is unprecedented in our time, there

is much contention regarding the best containment and mitigation strategies. As with most emerging infections, many preventive measures (e.g., vaccines) and curative approaches (e.g., drugs) are not yet available; therefore, countries must rely on non-pharmaceutical interventions—such as individual quarantine—to combat the illness.

Choosing the best intervention strategy is critical during an emerging epidemic, especially when uncertainties surround the disease and health systems are not adequately prepared. Public health officials often

initially employ contact tracing, wherein people possibly exposed to the disease become the focus of non-pharmaceutical interventions due to their enhanced risk. These contacts are promptly isolated if they are symptomatic. Often, however, they may appear uninfected when located. Depending on the time since exposure, these individuals might not yet be symptomatic—though they could develop symptoms in the future.

The best way to manage symptom-free contacts is highly disputed. History has relied upon two main strategies: individual quarantine and active symptom monitoring. Similar to isolation, individual quarantine involves the separation of potentially infected individuals from other people; this requires resources to provide necessities, access to secluded spaces, and means of enforcement. In contrast, active symptom monitoring allows individuals to essentially go about their normal routines while checking for symptoms at regular intervals, possibly with daily visits from healthcare workers or more technological-based self-monitoring. Under either intervention, patients are promptly isolated upon detection of symptoms. While individual quarantine is the more effective strategy by definition, it is also costlier and considerably more restrictive.

The success of these strategies relies on fundamental information about the disease's natural history: most importantly, the timing of when symptoms arise and when individuals are able to transmit the illness. The period between exposure and the onset of symptoms is known as the incubation period, while the period between exposure and infectiousness—i.e., the ability to transmit—is called the latent period (see Figure 1). For many illnesses, symptoms and infectiousness occur at roughly the same time; these two terms are therefore often confused. In order to determine which strategy is most appropriate for mitigating the spread of emerging infections, my colleagues and I built a framework to compare individual quarantine and active symptom monitoring approaches. Our model considers a range of feasibility parameters, including delays in contact tracing, imperfect isolation, and missed contacts [6]. As with many countries during the initial stages of COVID-19, insufficient or nonexistent testing capabilities may also hinder feasibility.

We used a discrete-time stochastic branching model—wherein individuals progress through a susceptible-exposed-infectious-recovered (SEIR) disease process—and focused on the early stages of an epidemic [6, 7]. We utilized data on distributions for the incubation period and serial interval to determine the timing of this progression. Once an individual was symptomatic and thus isolated, we traced a proportion of

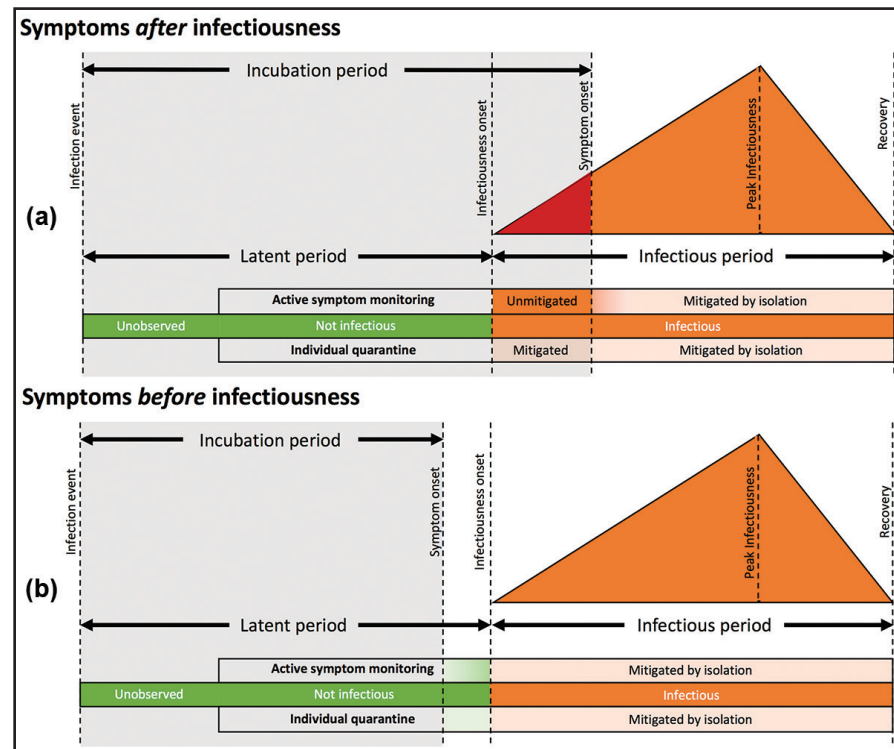


Figure 1. Timing of non-pharmaceutical interventions compared to disease progression. Following the infection event, individuals are noninfectious (green) until the onset of infectiousness, after which they can transmit the disease (orange). They are unobserved prior to and during contact tracing. Once an intervention—individual quarantine or active symptom monitoring—begins, individuals are isolated upon detection of symptoms. The gray area depicts the time before symptom onset. **1a.** For diseases where symptom onset occurs after the onset of infectiousness, individuals can transmit prior to isolation (red triangle). **1b.** For diseases where symptom onset occurs before infectiousness, no transmission is possible prior to isolation. Figure courtesy of Lauren Childs.

ISSN 1557-9573. Copyright 2020, all rights reserved, by the Society for Industrial and Applied Mathematics, SIAM, 3600 Market Street, 6th Floor, Philadelphia, PA 19104-2688; (215) 382-9800; siam.org. To be published 10 times in 2020: January/February, March, April, May, June, July/August, September, October, November, and December. The material published herein is not endorsed by SIAM, nor is it intended to reflect SIAM's opinion. The editors reserve the right to select and edit all material submitted for publication.

Advertisers: For display advertising rates and information, contact Kristin O'Neill at marketing@siam.org.

One-year subscription (nonmembers): Electronic-only subscription is free. \$73.00 subscription rate worldwide for print copies. SIAM members and subscribers should allow eight weeks for an address change to be effected. Change of address notice should include old and new addresses with zip codes. Please request address change only if it will last six months or more.

Editorial Board

H. Kaper, *Editor-in-Chief, Georgetown University, USA*
K. Burke, *University of California, Davis, USA*
A.S. El-Bakry, *ExxonMobil Production Co., USA*
J.M. Hyman, *Tulane University, USA*
O. Marin, *Argonne National Laboratory, USA*
L.C. McInnes, *Argonne National Laboratory, USA*
S. Minkoff, *University of Texas at Dallas, USA*
N. Nigam, *Simon Fraser University, Canada*
A. Pinar, *Sandia National Laboratories, USA*
R.A. Renaut, *Arizona State University, USA*

Representatives, SIAM Activity Groups

Algebraic Geometry
T. Crick, *Universidad de Buenos Aires, Argentina*
Analysis of Partial Differential Equations
G.G. Chen, *University of Oxford, UK*
Applied Mathematics Education
P. Seshaiyer, *George Mason University, USA*
Computational Science and Engineering
S. Rajamanickam, *Sandia National Laboratories, USA*
Control and Systems Theory
F. Leve, *Air Force Office of Scientific Research, USA*
Discrete Mathematics
D. Hochbaum, *University of California, Berkeley, USA*
Dynamical Systems
K. Burke, *University of California, Davis, USA*
Financial Mathematics and Engineering
A. Capponi, *Columbia University, USA*

Geometric Design

J. Peters, *University of Florida, USA*
Geosciences
T. Mayo, *University of Central Florida, USA*
Imaging Science
G. Kutyniok, *Technische Universität Berlin, Germany*
Life Sciences
M.A. Horn, *Case Western Reserve University, USA*
Linear Algebra
R. Renaut, *Arizona State University, USA*
Mathematical Aspects of Materials Science
K. Bhattacharya, *California Institute of Technology, USA*
Mathematics of Planet Earth
R. Welter, *Boston University, USA*
Nonlinear Waves and Coherent Structures
K. Oliveras, *Seattle University, USA*
Optimization
A. Wächter, *Northwestern University, USA*
Orthogonal Polynomials and Special Functions
P. Clarkson, *University of Kent, UK*
Uncertainty Quantification
E. Spiller, *Marquette University, USA*

SIAM News Staff

J.M. Crowley, *editorial director, jcrowley@siam.org*
L.I. Sorg, *managing editor, sorg@siam.org*

Printed in the USA.

SIAM is a registered trademark.

Obituary: Olvi L. Mangasarian

By Michael Ferris and Stephen Wright

Olvi L. Mangasarian, John von Neumann Professor Emeritus of Mathematics and Computer Sciences at the University of Wisconsin-Madison, passed away on March 15, 2020 due to complications from a fall and subsequent stroke. He was a pioneer, leader, and icon in the field of mathematical programming, with over 50 years of fundamental contributions to all aspects of continuous optimization—ranging from abstract theory to practical applications. Olvi’s work impacted generations of applied mathematicians and engineers, introduced new avenues of research, sparked excitement in applied subjects, and inspired countless young minds. His dedicated service to the Department of Computer Sciences at UW-Madison—and the broad applied mathematics community as a whole—exemplified the spirit and mission of a great academic.

Olvi was born in Baghdad, Iraq, in 1934. His parents were Armenian refugees who had fled the Armenian genocide in the Ottoman Empire in 1915. Olvi attended the Jesuit Baghdad College and American

University of Beirut before completing his final two years of undergraduate work on full scholarship at Princeton University, where he majored in civil engineering. He graduated from Princeton as a member of Phi Beta Kappa with a B.S.E. in 1954 and an M.S.E. in 1955. Olvi then studied applied mathematics at Harvard University, where he experienced the promise and frustrations of the emerging computer age. While at Harvard, he worked on the UNIVAC—a room-sized computer powered by vacuum tubes that continually required replacement—and used punch cards that at times cascaded helter-skelter across the floor. He received his Ph.D. from Harvard in 1959.

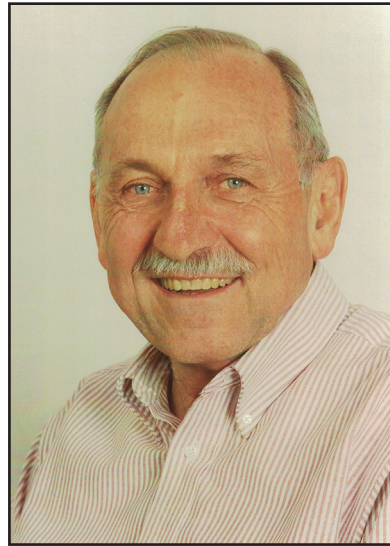
That same year, Olvi married Claire Garabedian, solidifying an alliance that

ended only with his passing. They first resided in Berkeley, Calif., where Olvi worked at Shell Development Company. In

1967, they moved to Madison, Wis., when Olvi joined the faculty of the Department of Computer Sciences at UW-Madison.

Early in his career, Olvi wrote a seminal paper on linear and nonlinear separation of patterns by linear programming. Published in 1965, this paper provided the foundation of the mathematical programming approach to data mining and knowledge discovery. Olvi revisited this subject in the late 1980s, amassing

a great following and cementing optimization’s fundamental role in the important applied domain of data science. As computing capabilities improved, he began explor-



Olvi L. Mangasarian, 1934-2020. Photo courtesy of Claire Mangasarian.

ing methods for data classification, which he employed to determine the malignancy of biopsied breast tissue samples. This effort ultimately yielded a remarkably successful decision support system that was used in clinical practice.

Olvi remained a central figure in continuous optimization throughout his career. One famous contribution, the Mangasarian-Fromovitz constraint qualification (MFCQ) for nonlinear programming (published in 1967), lies at the heart of constrained optimization. Subsequent research has indicated that the MFCQ can be extended to infinite-dimensional settings and is precisely the right condition to guarantee metric regularity—a form of regular behavior of the feasible set under the constraints’ deformations. It has thus enabled many subsequent advances in nonlinear programming.

In 1969, Olvi published *Nonlinear Programming*, a classic monograph that was reprinted in 1994 as part of SIAM’s *Classics in Applied Mathematics* series. This textbook remains an invaluable resource for students and a basic reference for researchers.

See Mangasarian on page 4

Global Outbreaks

Continued from page 1

a disease initially spreads with minimal hindrance, we can rely on the properties of exponential growth to guide us.

One common property of exponential growth that researchers frequently use for analysis is a disease’s doubling rate. This rate is the exponential mirror image of the logarithmic half-life and tells us how long it takes for the number of infections to double. The growth of COVID-19 has been quite aggressive in some countries, with a doubling time of as little as 1–2 days. For many countries, however, it takes 3–5 days for the number of cases to double. It is relatively simple to consider the population of a country and—assuming consistent exponential

growth—determine when that country will reach the critical density threshold of 1 confirmed case per 10,000 people.

The key assumption here is consistent exponential growth. In fact, few countries have exhibited a constant doubling time much past a week or two. Therefore, due to exponential growth’s sensitivity to initial conditions, we can only rely upon any prediction based on this technique for a week (or possibly two) ahead of the event.

Predicting a Slowing of Growth

Once we are in the midst of aggressive growth, what methods can we use to determine our progress? A common technique is to consider a log plot of the growth. If the curve is concave up, the doubling time is shortening and the disease is becoming

more aggressive. If the curve is flat, the disease is exhibiting consistent exponential growth and will eventually overwhelm the region. If the curve is concave down, growth is slowing and may be brought under control with time.

An alternative option involves determining where an illness has progressed on its characteristic curve. We can split the typical sigmoidal curve of a disease’s confirmed cases into three phases:

1. Exponential growth
2. Linear growth
3. Logarithmic flattening

By considering the best least-squares fit of these curves to the confirmed cases data, we gain an understanding of our status in terms of disease progress (see Figure 1, on page 1).

Utilizing this technique while accounting for the percentage of recovered cases allows us to define the moment when a country has recovered from disease. For example, with the slowing growth of new cases and the progressive increase in recoveries, the active cases (= confirmed cases – deaths – recoveries) follow a bell curve. By defining a percentage level of recovery, we can make predictions as to when this level is crossed.

Prediction in the Absence of Recovery Data

In March 2020, the Johns Hopkins Coronavirus Resource Center temporarily stopped releasing the numbers of recovered cases for countries of the world; the data was simply too unreliable. In the absence of recovery data, how else can we understand a country’s recovery?

One option is to reconsider the doubling time of COVID-19’s growth. Examining the doubling time’s daily trend yields a “fingerprint” of the disease and its progress. Figure 2 identifies a selection of countries and their doubling times through March 11, 2020. Each plot has a unique fingerprint, but some share common characteristics. For example, China and Singapore showed an increasing doubling time—i.e., a move to recovery—early on, although both countries experienced a setback in the middle of February before beginning to recover again.

South Korea and Italy both saw their first COVID-19 outbreaks in January and began to recover quickly until around February 20, when strong resurgences occurred. The countries both began recovering again over the next two weeks, but their ultimate outcomes have been quite different. By March 25, South Korea’s doubling time was over 20 days and the country was approaching a national recovery. Italy’s doubling time was about one third of South Korea’s, and the nation was far from recovering.

In contrast, the U.S. began recovering from its early outbreak but then underwent a setback towards the end of February. This new outbreak, presumably the one in the state of Washington, showed signs of an initial recovery but then grew out of control; the graph in Figure 2 dips again about a week later. Germany saw no strong recovery after its COVID-19 outbreak in late February and the doubling times have remained flat, which indicates ongoing exponential growth.

Lastly, Spain and the U.K. faced an initial outbreak at the start of February from which there was recovery, only to experience a secondary outbreak in the middle of the month. There was again recovery until a third wave at the end of February, from which both countries struggled to recover as quickly.

With the absence of recovery data, our definition of national recovery uses the duration of infection as the doubling time, since this implies that COVID-19 is well-controlled. Once a country has a doubling time of this length, we can consider it recovered. In the case of China, for example, a doubling time of 30 days correlated with around 80 percent of all patients having recovered or died.

What Did We Learn?

In summary, understanding the growth patterns of a fast-moving disease in the early stages of a pandemic is a challenging task. One-size-fits-all models are not appropriate, and long-term predictions—such as equilibrium values of differential equations, which use infinite time as a proxy for the distant future—are likely to be futile. Instead, adapting models to short-term data enables a deeper comprehension of the existing data while also allowing us to make predictions when data is unavailable.

Mathematics indicates that the fast-moving nature of COVID-19 necessitates fast-moving models. By determining crucial thresholds and adapting short-term “data fits,” modelling offers us a glimpse into the pandemic’s future across the world and clearly indicates that we must act as early as possible to mitigate spread. Even if this information comes too late for COVID-19, the lessons learned from this disease will apply to the next one. Infectious diseases will always be with us.

Leon Tribe holds an honours degree in mathematical physics and is head of data analytics at Tribe and Company, which is based in New South Wales, Australia. Robert Smith? (the question mark is part of his name) is a professor of disease modelling at the University of Ottawa, Canada.

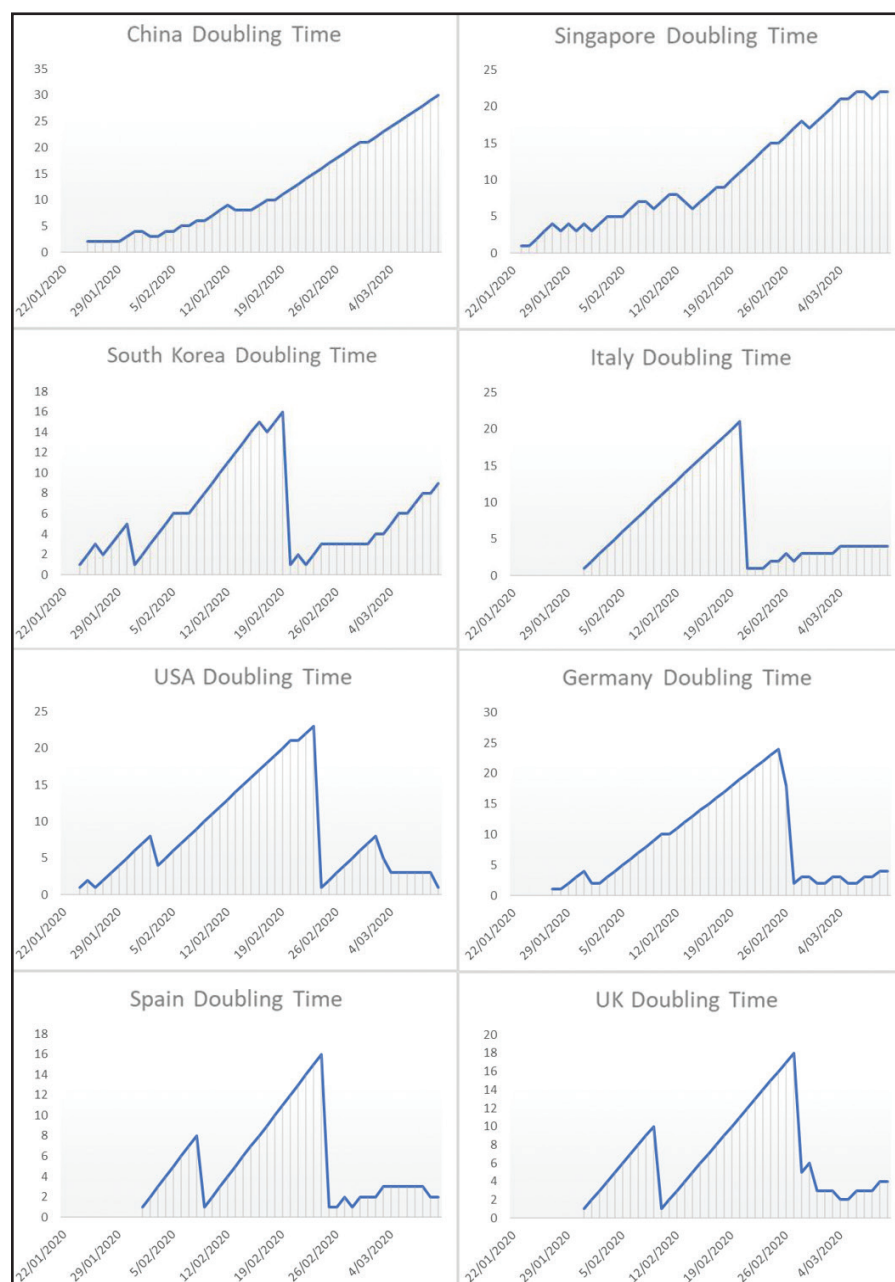


Figure 2. Doubling times of COVID-19 for a selection of countries. A higher (longer) doubling time is better. Figure courtesy of Leon Tribe.

Emerging Diseases

Continued from page 1

something to humans, then examine their features to try to understand what separates those with the capacity to infect humans from those without it.”

One complication is that reservoir species—rats, bats, monkeys, etc.—that harbor the pathogens often do not infect us directly. For instance, humans are infected with Zika virus via *Aedes* mosquito bites, but scientists think that the reservoir species is a type of monkey, thus making the mosquitoes disease *vectors* rather than reservoirs. In addition, the vector animals themselves may not be susceptible to zoonotic diseases; this means that they might harbor the pathogens and pass them to each other without getting sick, regardless of human vulnerability.

Identification of reservoir species has faced its share of successes and failures. For example, researchers have linked rodents to both Lyme disease and the plague and implicated bats in diseases such as rabies, the Nipah virus, and possibly Ebola. We know that monkeys are probably reservoirs for the Zika virus and bats almost certainly harbored the coronavirus that caused the 2003 SARS epidemic. However, the evidence is circumstantial.

Han and her colleagues identified five primary predictive factors that make species potential reservoirs for zoonotic pathogens: litter size (θ_1), the number of litters each species has per year (θ_2), maximum longevity (θ_3), population density (θ_4), and social group size (θ_5). Physical characteristics like body size correlate with many of these properties; for instance, small rodents have many tiny offspring and often live in very high-density conditions that facilitate transmission of pathogens between animals.

During her AAAS talk, Han described these parameters’ use in a modified version of the classic SIR model for epidemics:

$$\frac{dS}{dt} = b_0N - b_1N^2 - \beta SI - \mu S$$

$$\frac{dI}{dt} = \beta SI - (\gamma + \mu)I$$

$$\frac{dR}{dt} = \gamma I - \mu R,$$

where $N(t) = S + I + R$ is the total local population of a rodent species and S , I , and R respectively denote the number of susceptible, infected, and recovered animals. She derives the fixed parameters from the species characteristics: birth rate $b_0 = \theta_1\theta_2$, death rate $\mu = \theta_3^{-1}$, and population density parameter $b_1 = (b_0 - \mu)/\theta_4$. The variable parameters are recovery rate $1/2 < \gamma^{-1} < \theta_3$ and transmission probability $0.1\theta_5 < \beta < \theta_5$, which one can adjust to suit the specific population under consideration (the standard SIR model can be recovered by setting $b_0 = b_1 = \mu = 0$, which implies a constant population N).

In addition to species characteristics, the frequency of contact between humans and animals is a major factor. “You do not have a transmission event unless there is some opportunity for that pathogen to get to you,”

Han said. “When humans encroach on wild lands, or prevent animals from accessing food resources so they have to forage in different places, these things all contribute to increased contact frequency with people.”

Changes in human behavior—including deforestation, widespread urbanization, disruption of traditional hunting patterns, and so on—can also introduce contact with species to which we are unaccustomed. These alterations to human-animal interactions mean that people hunt animals they typically did not in the past, or share living space with novel species. To put it another way: while bats may harbor SARS-CoV-2, a cascade of human behaviors brought our species into collision and transformed limited exposure into a global pandemic.

The Hole in the Doughnut

However, scientists can seldom immediately link a zoonotic outbreak to contact with another species, particularly when a vector or other intermediary species is involved — as with the 2003 SARS outbreak, where a civet was likely the carrier that infected the first humans. “We’re still clambering for information on primates,” Han said, referring to her own work to identify the source of the recent devastating Zika epidemic in the Americas. “Without understanding the reservoir’s biology, how can you make an accurate prediction that’s going to help you take preventative action?”

When a paucity of information exists about a species, epidemiologists become detectives. To identify potential reservoirs for the Zika virus, Han and her collaborators tabulated 33 parameters for 364 primate species (not counting humans). These traits included those used for rodents but also comprised geographic range, metabolic rate, and other potentially useful information. At least one parameter was unknown for over a third of the primates, so the group applied an iterative method called multiply imputed chained equations (MICE) to estimate values for these species. Since the relationship between parameters is not entirely random within species—for example, small species do not normally produce multiple large offspring—and similar species often possess similar characteristics, the MICE method employs regression to fill in the missing information in a biologically consistent manner [1].

But species parameters are not enough; the hole in the doughnut inside the other doughnut is whether a given species is the reservoir for a zoonotic disease. To estimate this probability, Han and her team utilized Bayesian Multi-label Learning via Positive Labels (BMLPL) [3]. This method assigns binary labels to each species, specifically asking whether animals carry a given virus. The answer might be known for certain species, such as monkeys that are affirmatively tested to carry the Zika or dengue virus. The group’s analysis involved six flaviviruses (the type including Zika, dengue, and West Nile) and the aforementioned 364 types of primates.

The training data for BMLPL are a matrix \mathbf{X} composed of the known parameters and those obtained via MICE. The “label” matrix \mathbf{Y} consists of 0 and 1 values—depending on whether a given species carries a particular virus—for each of the six viruses under consideration. Since this information is unknown for most of the 364 species, \mathbf{Y} is a very sparse matrix. However, related species are more likely to harbor similar viruses, so the entries are not random in general. The BMLPL method takes in the vector of parameters for a species \mathbf{x} from \mathbf{X} and uses machine learning to extract a label vector \mathbf{y} from \mathbf{Y} .

These coupled methods allowed Han and her colleagues to identify primate reservoirs for flaviviruses with 82 percent accuracy. They also found that these reservoirs were the most likely to live near or among humans. However, Han pointed out that reconstructing missing parameters can only go so far. “I think we are quickly heading

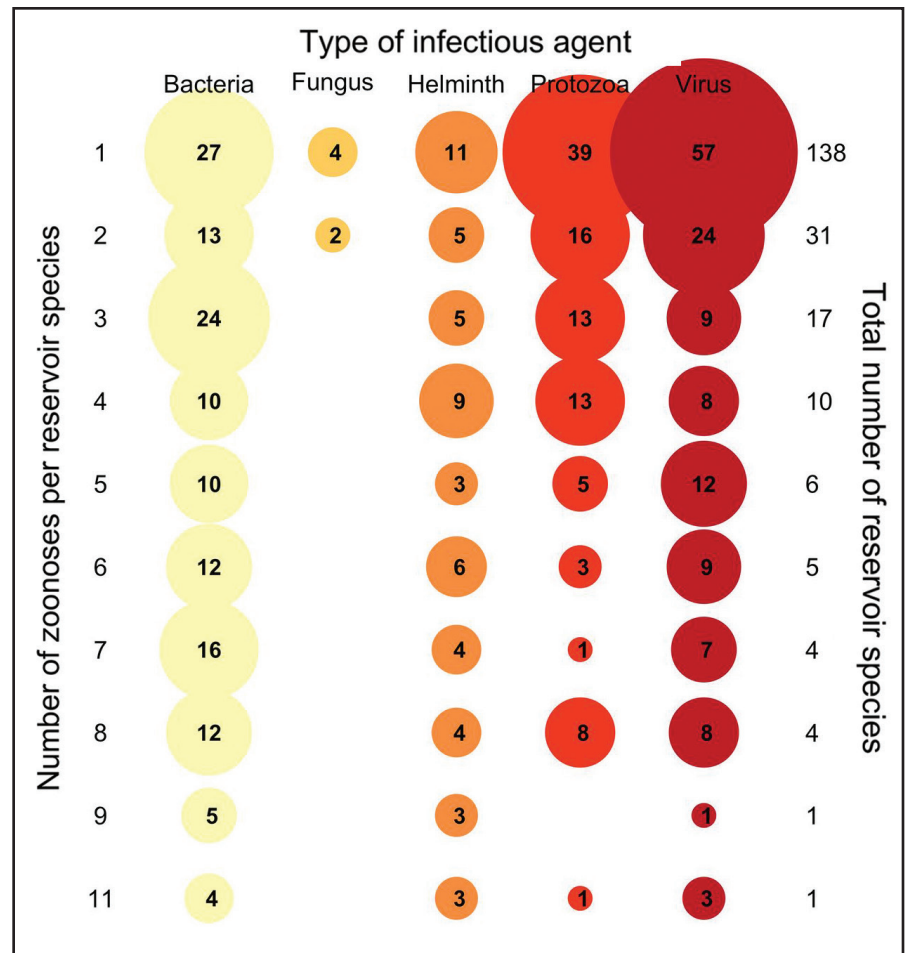


Figure 1. Prevalence of known zoonotic pathogens and their distribution among rodent species. Most classified pathogens are viruses and most species only harbor one type that is known to be harmful to humans. Figure courtesy of [2].

towards a wall of just not having the kind of available data that we need,” she said. “There must be equal investment in generating the raw data required for useful, actionable, and accurate predictions. Without that, we cannot move forward.”

This is certainly a common refrain in the context of novel diseases, wherein we are hampered by the fact that obtaining data from noisy, real-world situations takes time. It is not enough to say that bats are the reservoir for a disease, or that *Aedes* mosquitoes carry Zika virus. We must know what specific human-animal interactions turn zoonotic infections into epidemics and learn how to mitigate them. Even the best detectives can only do so much; they need evidence in order to work.

References

- [1] Han, B.A., Majumdar, S., Calmon, F.P., Glicksberg, B.S., Horesh, R., Kumar, A., ..., Varshney, K.R. (2019). Confronting data sparsity to identify potential sources

of Zika virus spillover infection among primates. *Epidem.*, 27, 59.

[2] Han, B.A., Schmidt, J.P., Bowden, S.E., & Drake, J.M. (2015). Rodent reservoirs of future zoonotic diseases. *Proc. Natl. Acad. Sci.*, 112, 7039.

[3] Rai, P., Hu, C., Henaou, R., & Carin, L. (2015). Large-scale Bayesian multi-label learning via topic-based label embeddings. In C. Cortes, N.D. Lawrence, D.D. Lee, M. Sugiyama, & R. Garnett (Eds.), *Advances in neural information processing systems 28 (NIPS 2015)* (pp. 3222-3230). Montreal, Canada: Curran Associates, Inc.

Further Reading

Quammen, D. (2012). *Spillover: Animal infections and the next human pandemic*. New York, NY: W.W. Norton & Company.

Matthew R. Francis is a physicist, science writer, public speaker, educator, and frequent wearer of jaunty hats. His website is BowlerHatScience.org.

Mangasarian

Continued from page 3

Olvi achieved numerous fundamental results throughout his career, most notably in the areas of linear and nonlinear programming, complementarity problems, variational inequalities, error bounds for inequality systems, and parallel optimization. His work is known for its elegance, enormous impact, and foundational role in copious subsequent extensions.

From 1970 until about 1990, Olvi and several colleagues (including Ben Rosen, Stephen Robinson, and Robert Meyer) organized a series of conferences in Madison, Wis., first on nonlinear programming and later on parallel optimization. These meetings were important events in their fields and attracted top researchers from around the world, as well as junior researchers and students. They inspired the introduction and discussion of many exciting ideas and are remembered vividly by those who participated.

During his time at UW-Madison, Olvi mentored 28 Ph.D. students and was chair of the Department of Computer Sciences for three years. Following his retirement from the university, Olvi spent the winter months in San Diego, Calif., where he worked as a research scientist at the University of California, San Diego.

From 1969-1984, Olvi served on the editorial boards of the *SIAM Journal on Control and Optimization* and *SIAM Journal on Optimization*. He was a correspond-

ing editor from 1985-1993. Olvi became a SIAM Fellow in 2011 and was recognized for his efforts to advance the application of mathematics to science and industry. He also received the 2000 Frederick W. Lanchester Prize from INFORMS for his research on machine learning and data mining, among other honors.

Olvi’s love of classical music began in his college years and continued throughout his life. Like many mathematicians, he was partial to the Baroque period. Johann Sebastian Bach topped his playlist, and concerts at the Wisconsin Union Theater were a particular delight.

Olvi was an inspirational person who will be greatly missed by the Department of Computer Sciences at UW-Madison, which he helped shape over many years of service, and by his many friends and admirers in the optimization community. He is survived by his wife Claire; sons Leon, Jeffrey, and Aram; and six grandchildren.

This obituary was adapted in part from a tribute¹ by the Department of Computer Sciences at the University of Wisconsin-Madison, which published in March.

Michael Ferris and Stephen Wright are professors in the Department of Computer Sciences at the University of Wisconsin-Madison.

¹ <https://www.cs.wisc.edu/2020/03/20/olvi-mangasarian-emeritus-professor-and-pioneer-in-mathematical-programming-passed-away-march-15>

Want to Place a Professional Opportunity Ad or Announcement in SIAM News?

Please send copy for classified advertisements and announcements in *SIAM News* to marketing@siam.org.

For details, visit www.siam.org/advertising.

Check out the SIAM Job Board at jobs.siam.org to view all recent job postings.

Math and AI-based Repositioning of Existing Drugs for COVID-19

By Duc D. Nguyen and Guo-Wei Wei

Coronavirus disease 2019 (COVID-19), an infectious disease caused by severe acute respiratory syndrome coronavirus 2 (SARS-CoV-2), was first reported in Wuhan, China, in December 2019 and has rapidly spread throughout the world. By April 2, 2020, COVID-19 had infected more than one million individuals and was responsible for over 50,000 fatalities. No specific antiviral drug for this pandemic currently exists.

Drug discovery involves target discovery, lead discovery, lead optimization, preclinical development, three phases of clinical trials, and an eventual market launch — only if everything goes well. On average, bringing a new drug to market requires about \$2.6 billion dollars and over 10 years of preparation. It typically takes researchers more than a year to develop effective viral vaccines.

Drug repositioning (also known as drug repurposing)—which involves the investigation of existing drugs for new therapeutic target indications—is one of the most feasible strategies for treating COVID-19 patients. It has emerged as a successful way to accelerate drug discovery due to the reduced costs and expedited approval

procedures [7]. Several successful examples unveil the value of drug repositioning. Nelfinavir, which was initially developed to treat human immunodeficiency virus (HIV), is now used for cancer treatments. Researchers first designed amantadine to combat the type A influenza viral infection, but it is presently used to treat Parkinson's disease. And remdesivir, an experimental drug initially developed to inhibit Middle East Respiratory Syndrome, is being repurposed for COVID-19.

In recent years, the rapid growth of drug-related datasets and open data initiatives has inspired new developments for computational drug repositioning, particularly structural-based drug repositioning (SBDR). Machine learning (ML), network analysis, and text mining and semantic inference are three major computational approaches that researchers commonly apply to drug repurposing [7]. Swift accumulation of genetic and structural databases, development of low-dimensional mathematical representations of complex biomolecular structures [10], and availability of advanced deep learning algorithms have made ML-based drug repositioning one of the most promising approaches for COVID-19 [7].

The first step of SBDR is the selection of one or several effective targets. Studies show that the SARS-CoV-2 genome is very close to that of the early SARS-CoV. The sequence identity percentages of the SARS-CoV-2 main protease, RNA polymerase, and spike protein with those of corresponding SARS-CoV proteins are 96.08, 96, and 76, respec-

tively. The catalytic sites of the SARS-CoV main protease are very conservative and serve as attractive therapeutic targets. Therefore, a potent inhibitor of this protease is likely a potent inhibitor of the SARS-CoV-2 main protease. Unfortunately, there is also currently no effective SARS-CoV therapy.

See AI-based Repositioning on page 8

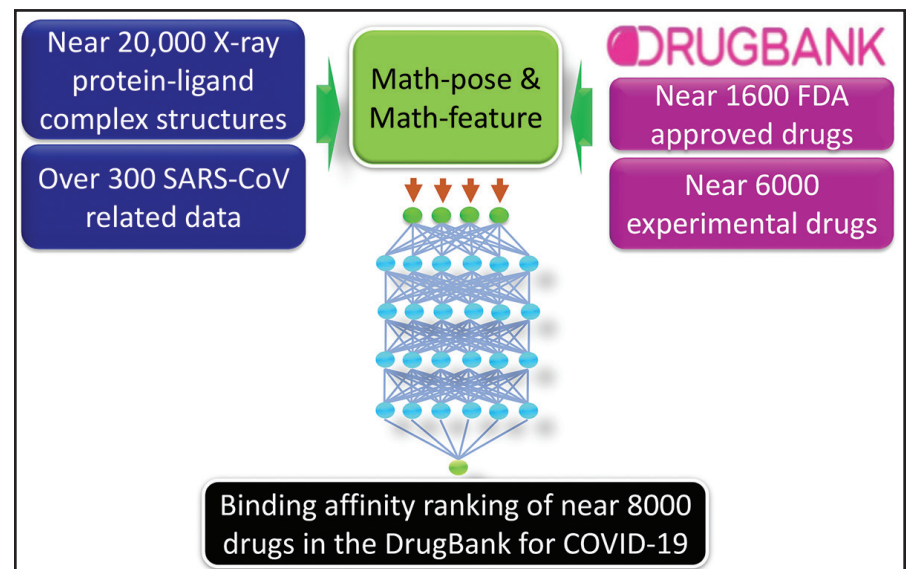


Figure 1. Flow chart of mathematics and artificial intelligence (AI)-based COVID-19 drug repositioning. Figure adapted from [12].

Intervention Strategies

Continued from page 2

his/her contacts with a time lag that accounts for the possibility of delays — as would occur during a real epidemic. While infectious, patients generate new infections following a negative binomial distribution with a dispersion parameter that allows for variability in infectiousness [6, 8]. The basic reproductive number (R_0) and the fitted distribution of infectiousness dictate the number of new infections in a given time period. Based on published results for distributions of the incubation period and serial interval, we used particle filtering—i.e., a sequential Monte Carlo algorithm—to fit the maximum duration of infectiousness, time of peak infectiousness, and time offset between the incubation and latent periods.

This framework allowed us to examine the extent to which individual quarantine and active symptom monitoring can mitigate or control an epidemic; we do so by determining the effective reproductive numbers (R_{eff}) under each intervention in high and low feasibility settings [6]. For diseases where symptoms emerge prior to or at the onset of infectiousness—like Ebola, pertussis (whooping cough), SARS, and Middle East respiratory syndrome—individual quarantine yields little additional benefit over active symptom monitoring. However, the absolute ability to control a disease, i.e., driving $R_{\text{eff}} < 1$, under either scenario is a combination of the basic reproductive number and the feasibility setting. For example, pertussis was uncontrollable with either strategy when $R_0 = 5$, though R_{eff} fell

below 2 with both non-pharmaceutical interventions. In contrast, short-course illnesses (such as influenza A) or those with extensive pre-symptomatic infectiousness (such as Hepatitis A) showed significantly greater impacts with individual quarantine. In a high feasibility setting where contact tracing and isolation are effective, R_{eff} fell below 0.5 with individual quarantine but remained above 1 for active symptom monitoring.

In the ongoing COVID-19 epidemic, a key uncertainty is the extent of transmission that occurs when individuals do not display symptoms. The incidence of pre-symptomatic or asymptomatic cases of COVID-19 inspired considerable debate in the community when an early study reporting pre-symptomatic transmission later came into question [9]. Furthermore, reported serial intervals—the time between symptom onset of an infector and symptom onset of an infectee—have varied considerably. We utilized two published estimates of the serial interval: one short (mean of 4.8 days) and one longer (mean of 7.5 days) [4, 5]. Model results using data from the shorter interval indicate that the mean time of infectiousness is nearly a day prior to symptom onset, suggesting considerable pre-symptomatic transmission [7]. We found the mean time of infectiousness using the longer serial interval to be shortly after symptom onset, although a period of pre-symptomatic transmissibility remains.

By employing our framework and parameter estimations, we determined that in high feasibility settings—where most contacts are traced with minimal delay and isolation is nearly perfect—individual quarantine can

drive down transmission in more than 95 percent of scenarios [7]. Comparatively, active symptom monitoring reduces R_{eff} below 1 only 12 percent of the time. Low feasibility settings—where about half the contacts are traced, isolation is moderately effective, and longer delays for tracing and treatment exist—cannot sufficiently achieve control with either individual quarantine or active symptom monitoring. Our work assumed current estimates of the basic reproductive number of COVID-19: $R_0 = 2.2$ [4, 8]. However, control was impossible even when reducing R_0 to 1.5. The inability for disease containment in these cases stems from the fact that many transmission chains are not followed at all, not followed quickly enough, or incompletely stopped to prevent additional spread. Nonetheless, onward transmissions can be blocked for an individual whose contacts are traced, therefore reducing overall burden within the population. Thus, even in situations where containment is inconceivable with individual quarantine and active symptom monitoring, these strategies will help mitigate transmission and can be used in conjunction with other policies.

To more adequately track the burden of individual quarantine in the COVID-19 outbreak, we also considered a fraction of ultimately uninfected but traced contacts who self-quarantine for 14 days—the current recommendation [1, 2]—before returning to normal activities. Thus, the number of individuals under quarantine grows significantly more quickly than the number of cases (see Figure 2) and is likely to rapidly outpace available resources. In these situations, people must exercise more general interventions like mass quarantine, travel restrictions, or social distancing. However, it is important to note that such interventions also depend on our understanding of a disease's natural history. With COVID-19, which shows evidence of pre-symptomatic transmission, mass quarantine—as occurred on the Diamond Princess cruise ship—forced infected and uninfected individuals to remain together in close quarters and may have led to additional cases.

Contact tracing and the resulting non-pharmaceutical interventions, like individual quarantine and active symptom monitoring, have the potential to be quite effective in combatting certain types of infectious diseases. The extent of each strategy's efficacy depends on assumptions pertaining to the underlying parameters, such as serial interval, incubation period, and feasibility setting. In some circumstances, particularly when symptoms arise before infectiousness, both approaches may adequately eliminate the disease. In other scenarios, as appears

to be the case in the ongoing COVID-19 pandemic, use of these measures alone is insufficient. Nevertheless, individual quarantine and active symptom monitoring do mitigate spread and can complement social distancing and travel restrictions.

References

- [1] Centers for Disease Control and Prevention. (2020). *Interim U.S. guidance for risk assessment and public health management of persons with potential 2019 novel coronavirus (2019-nCoV) exposure in travel-associated or community settings*. Retrieved from <https://stacks.cdc.gov/view/cdc/84776>.
- [2] Chinese Center for Disease Control and Prevention. (2020). *COVID-19 prevention and control guidelines*. Retrieved from <http://www.nhc.gov.cn/jkj/s3577/202003/4856d5b0458141fa9f376853224d41d7/files/4132bf035bc242478a6eaf157eb0d979.pdf>.
- [3] Dong, E., Du, H., & Gardner, L. (2020). An interactive web-based dashboard to track COVID-19 in real time. *Lancet Infect. Dis.* To be published.
- [4] Li, Q., Guan, X., Wu, P., Wang, X., Zhou, L., Tong, Y., ..., & Feng, Z. (2020). Early transmission dynamics in Wuhan, China, of novel coronavirus — infected pneumonia. *New Eng. J. Med.*, 382(13).
- [5] Nishiura, H., Linton, N.M., & Akhmetzhanov, A.R. (2020). Serial interval of novel coronavirus (COVID-19) infections. *Int. J. Infect. Dis.*, 4(93), 284-286.
- [6] Peak, C.M., Childs, L.M., Grad, Y.H., & Buckee, C.O. (2017). Comparing non-pharmaceutical interventions for containing emerging epidemics. *Proceed. Nat. Acad. Sci.*, 114(15), 4023-4028.
- [7] Peak, C.M., Kahn, R., Grad, Y.H., Childs, L.M., Li, R., Lipsitch, M., & Buckee, C.O. (2020). Modeling the comparative impact of individual quarantine vs. active monitoring of contacts for the mitigation of COVID-19. *Lancet Infect. Dis.* To be published.
- [8] Riou, J., & Althaus, C.L. (2020). Pattern of early human-to-human transmission of Wuhan 2019 novel coronavirus (2019-nCoV), December 2019 to January 2020. *Eurosurveill.*, 25(4).
- [9] Rothe, C., Schunk, M., Sothmann, P., Bretzel, G., Froeschl, G., Wallrauch, C., ..., & Hoelscher, M. (2020). Transmission of 2019-nCoV infection from an asymptomatic contact in Germany. *New Eng. J. Med.*, 382, 970-971.

Lauren M. Childs is an assistant professor of mathematics at Virginia Tech, where she develops and analyzes mathematical and computational models that examine biologically-motivated questions. Understanding the pathogenesis and spread of infectious diseases, such as malaria and dengue, is a main focus of her work.

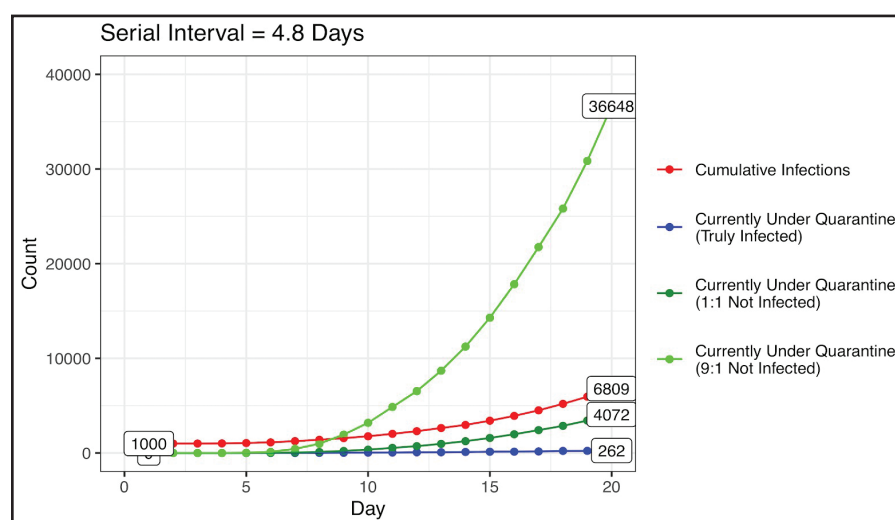


Figure 2. Simulated number of cumulative infections and individuals currently under quarantine. The daily count of cumulative infections is shown in red and the known infected contacts currently under quarantine appear in blue. Uninfected contacts currently under quarantine that assume a 1:1 ratio of uninfected to infected contacts traced are in dark green, and uninfected contacts currently under quarantine that assume a 9:1 ratio of uninfected to infected contacts traced are in light green. Quarantine is imposed when the cumulative case count reaches 1,000. These results assume a low feasibility setting, a basic reproductive number $R_0 = 2.2$, and a shorter mean serial interval of 4.8 days. Figure courtesy of [7].

Looking Ahead to the 2021 SIAM Conference on Computational Science and Engineering

By Laura Grigori, Misha E. Kilmer, and Stefan M. Wild

Interested in participating in a SIAM conference? The 2021 SIAM Conference on Computational Science and Engineering (CSE21),¹ to be held March 1-5, 2021 in Fort Worth, Texas, is an ideal venue for presenting your work and networking with colleagues.

If you are an applied mathematician, computer scientist, domain scientist, or engineer—and if your research is related to the theory, development, or use of computational technologies for the solution of problems in science and engineering—the biennial CSE conference is for you. CSE21 is expected to be SIAM's largest meeting to date, which is unsurprising given the interdisciplinary nature of computational science and engineering and the broad impact of research in this area. The organizing committee has designed CSE21 to highlight trailblazing activities and research that you will not want to miss.

The committee has reformatted the conference to encourage broader community participation and deeper attendee interactions. Highlights include the following:

- Six minitutorials that span the week and cover software and computing tools from around the world

¹ <https://www.siam.org/conferences/cm/program/cse21>

- Action-packed poster sessions that feature the return of e-posters, plenary poster blitzes, and cash prizes for poster awards

- Exciting panels intended for all career levels and research and development support worldwide

- Plenary talks on state-of-the-art research across the CSE landscape

- Contributed lectures integrated with fast-paced minisymposia

- An end-of-conference award ceremony with lectures from prize recipients.

The Broader Engagement (BE) program² will be present at the conference for the fourth time and seeks to expand the CSE community by supporting individuals from diverse backgrounds while simultaneously catalyzing change to create a more inclusive and diverse society. The program helps participants develop a sense of belonging through an orientation session, occasions for mentorship, and motivational workshops and other activities. To support technical growth (and in addition to CSE21's technical program), BE includes small learning groups called "Guided Affinity Groups,"³ entry-level tutorials, and career and professional development sessions. Volunteer

² <http://shinstitute.org/siam-cse21-broader-engagement-program/>

³ <http://shinstitute.org/guided-affinity-groups-for-be-cse21/>

opportunities⁴ are also available for the CSE community. All conference attendees are welcome to come to BE sessions and participate in the BE program.

Themes of CSE21 include traditional hot topics such as multiscale, multiphysics, and multilevel methods, as well as emerging research areas like quantum algorithms, computation, and information science. Presentations will also address the mathematics of artificial intelligence and machine learning.

While we strongly encourage proposals for minisymposia, posters, and contributed talks in areas that relate to the CSE21 themes, we welcome participation from anyone whose research falls within the broad scope of the field. Submissions in all forms are currently open.⁵

Opportunities for employers and institutions to sponsor CSE21 activities or participate in a daylong career fair are also currently available. Sponsorship forms are accessible on the conference page.⁶

Neither SIAM membership nor membership in the SIAM Activity Group on

⁴ <http://shinstitute.org/siam-cse21-broader-engagement-volunteer-opportunities/>

⁵ <https://www.siam.org/conferences/cm/submissions-and-deadlines/cse21-submissions-deadlines>

⁶ <https://www.siam.org/Portals/0/Conferences/CSE21/CSE21%20Sponsor%20Form.pdf>

Computational Science and Engineering (SIAG/CSE) is required for conference registration. However, SIAM members will receive a discounted registration fee and members of the SIAG/CSE are entitled to an additional discount.

CSE21 promises to facilitate in-depth technical discussions pertaining to a wide variety of major computational efforts on large-scale problems in science and engineering. The meeting will foster the interdisciplinary culture necessary to meet these challenges and promote the training of the next generation of computational scientists. We hope to see you in Fort Worth!

Laura Grigori, Misha E. Kilmer, and Stefan M. Wild are co-chairs of the organizing committee for the 2021 SIAM Conference on Computational Science and Engineering. Laura Grigori is a senior research scientist at Inria and Sorbonne University, France, as well as a SIAM Fellow. Misha E. Kilmer is William Walker Professor of Mathematics at Tufts University. She is also a SIAM Fellow. Stefan M. Wild is a computational mathematician in the Laboratory for Applied Mathematics, Numerical Software, and Statistics at Argonne National Laboratory. He is a Senior Fellow at Northwestern University's Northwestern Argonne Institute of Science and Engineering.

Modeling the Spread of COVID-19

By David I. Ketcheson

In the last several months, the rapid spread of COVID-19—the disease caused by the novel severe acute respiratory syndrome coronavirus 2 (SARS-CoV-2)—has turned our daily lives upside down. As of early April, the number of confirmed cases was well over one million, with the number of total infections certainly much higher. But these numbers are small compared to what we know will come. This is because the virus's spread is a classic example of exponential growth, in which the increase of some quantity (in this case, the infected population) is proportional to its current size. Infectious diseases grow exponentially because each newly-infected person becomes another source of infection.

One of the simplest epidemiological models is the SIR model [3]. It divides the population into three groups:

- Susceptible individuals (S), who have not yet been infected
- Infectious individuals (I), who are infected and can infect others
- Recovered individuals (R), who were previously infected and are now immune.

The model takes the form of three differential equations that describe the rates at which individuals transition between these groups:

$$\frac{dS}{dt} = -\beta IS$$

$$\frac{dI}{dt} = \beta IS - \gamma I$$

$$\frac{dR}{dt} = \gamma I.$$

$S(t)$, $I(t)$, and $R(t)$ are the respective fractions of the population in the susceptible, infectious, and recovered groups. We assume that people randomly come into contact with each other at a rate of β encounters per person per day. Each time an infectious person encounters a susceptible person, the virus spreads. Meanwhile, $1/\gamma$ is the average infectious period. Thus, if a single individual is initially infectious, he/she will pass the disease to $R_0 = \beta/\gamma$ other people on average. R_0 is called the *basic reproduction number* and is a property of both the disease and the behavior of the population in which it propagates.

Figure 1 depicts the typical spread of a new disease in a completely susceptible population. Since initially $S \approx 1$ and $I, R \ll 1$, we observe exponential growth as predicted by the second differential equation:

$$I'(t) \approx (\beta - \gamma)I(t),$$

whose approximate solution is $I(t) = \exp((\beta - \gamma)t)$. If $\beta < \gamma$, the infectious

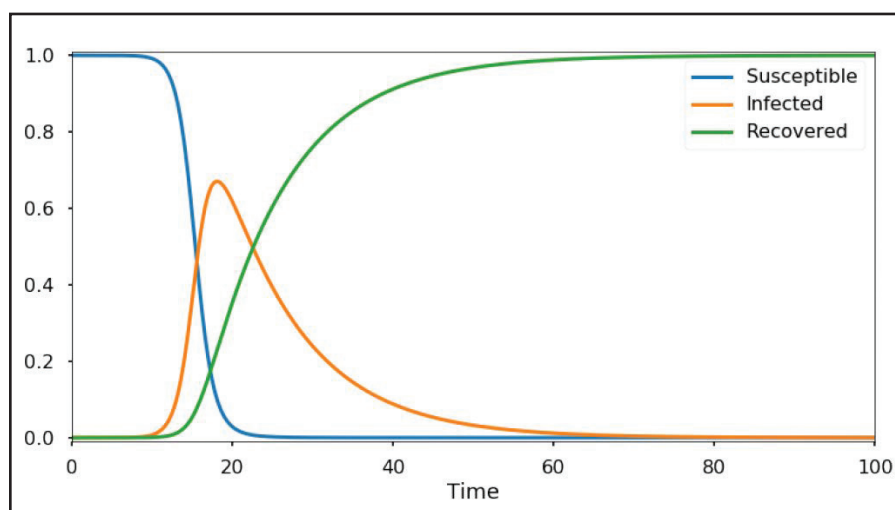


Figure 1. Typical SIR (susceptible-infectious-recovered) model behavior.

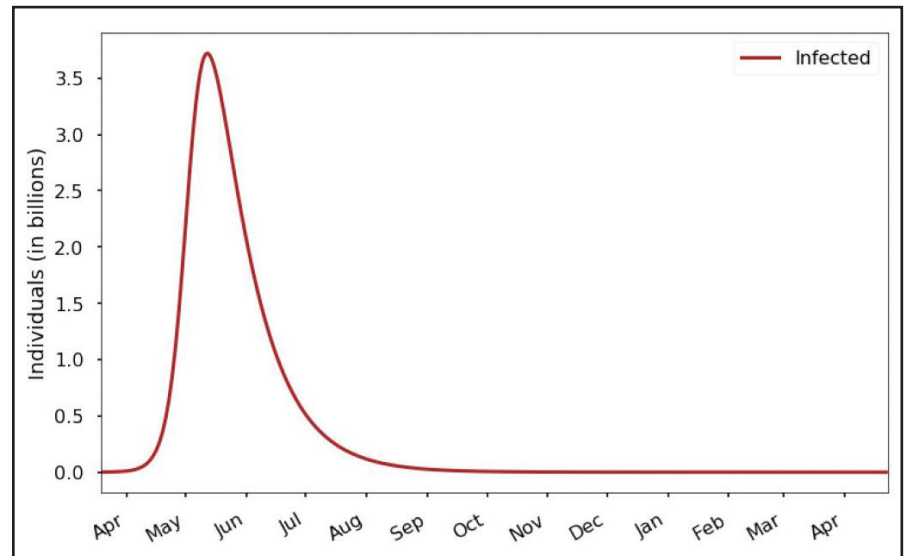


Figure 2. Predicted spread of COVID-19 in the absence of intervention.

population will decrease; this makes sense because $R_0 < 1$ in this case, meaning that each infected individual passes the disease to less than one other person on average. But if $\beta > \gamma$, the number of infected people will double over each time interval of length

$$t_d = \frac{\ln(2)}{\beta - \gamma},$$

which is known as the *doubling time*. This exponential growth will eventually slow as the susceptible population S decreases. We reach the peak in the infectious population when $I'(t) = 0$, i.e., when $\beta S = \gamma$ or $S = 1/R_0$.

Although the SIR model is simple, it is a surprisingly powerful tool for both qualitative and quantitative predictions in the real world [2]. However, it is notoriously difficult to determine the model parameters β , γ —or equivalently, R_0 and t_d —for a new disease while the epidemic is still growing. Early approximations of R_0 for COVID-19 ranged from about 2.5 to as low as 1.4, but more recent estimates put R_0 closer to 4. Measured values of the doubling time have ranged from two days to one week, with typical values of roughly three-four days.

Figure 2 displays the results of modeling COVID-19's spread on a global scale with these parameters. The natural consequence of rapid proliferation within a completely susceptible population is a pandemic that peaks during the summer and infects the great majority of humankind. Although most cases of COVID-19 are mild or asymptomatic, it is clear that this scenario would completely overwhelm the health-care systems in every country for at least several weeks during the peak of the crisis.

Equilibrium

The SIR model is at equilibrium if and only if $I = 0$, since all terms on the right-hand side of the system are proportional to I . If this equilibrium is stable, a small local outbreak will not spread. But if it is unstable, any small outbreak will become a global epidemic. Eigenvalue analysis confirms what we have already observed: the zero-infection equilibrium is stable if and only if $S \leq 1/R_0$. This means that a certain fraction of the population *must* catch the disease before it will die out; that fraction is $(R_0 - 1)/R_0$. This intuitively makes sense. For instance, suppose that R_0 is 4. In a fully susceptible population, each infected person will infect about four other

Spread of COVID-19

Continued from page 6

people. But if three-fourths of the population is already recovered and thus immune, then one infectious individual will only pass the disease to one new susceptible individual on average. This notion is called *herd immunity*. An individual who is still susceptible but lives in a society that is largely immune to a given illness is very unlikely to catch that illness because of the stability of the zero-infection equilibrium. In fact, the fraction of people who will eventually become infected is greater than $(R_0 - 1)/R_0$, since that is simply the point at which the equilibrium stabilizes.

The system still must reach this equilibrium, and along the way many more cases will emerge. The number of excess infections is known as *epidemiological overshoot*.

Intervention

The basic SIR model assumes that the contact rate β is constant in time. But as with COVID-19, a threatened population may change its behavior in an effort to reduce the rate of contact and slow or halt a disease's spread. This is the goal of the current widespread school and work closures, stay-at-home directives, and other restrictive social distancing measures. The medical literature refers to such phenomena as *non-pharmaceutical interventions*. If we denote the fraction of contact prevented through intervention as $q(t)$, we can include it in the SIR model as follows:

$$\frac{dS}{dt} = -(1 - q(t))\beta IS$$

$$\frac{dI}{dt} = (1 - q(t))\beta IS - \gamma I$$

$$\frac{dR}{dt} = \gamma I.$$

In the absence of intervention, we have $q=0$. In contrast, putting each person in complete isolation yields $q=1$. Real-world interventions lie somewhere between these two extremes.

Increasing the value of q has the same effect as decreasing β , in that it both slows the rate of exponential growth—stretching the epidemic over a longer time period—and lowers the peak. We now see that the zero-infection equilibrium is stabilized when $(1 - q(t))S(t) \leq 1/R_0$. Considering our example value of $R_0 = 4$, reducing contact by 50 percent means that only half of the population must now get infected before the epidemic will begin to subside. Figure 3 (on page 1) illustrates these effects, which reflect the now-well-known phrase of “flattening the curve.”

One consequence of exponential growth is that interventions are most effective when they are imposed before an epidemic becomes widespread. For instance, a study of the 1918 Spanish flu pandemic found that reduced peak rates of infection strongly correlated with how early a community imposed intervention measures [1].

Exit Strategy

We must remember that the aforementioned reduced criterion for equilibrium holds only as long as the intervention persists. When a community reverts to its pre-intervention lifestyle, $q(t)$ returns to 0. It is extremely difficult to completely eliminate a virus on a global scale, and a new epidemic will emerge if the susceptible fraction of the population is higher than $1/R_0$. This type of resurgence occurred in many U.S. cities during the 1918 Spanish flu epidemic — especially in locations where strong, early interventions were imposed. Figure 4 depicts an example of this scenario for COVID-19.

At the moment, humankind is more or less unified in a colossal effort to drive the spread of COVID-19 to an artificial and temporary equilibrium. In the short term, this effort seems necessary to prevent the disease from completely overwhelming healthcare systems. But the long-term strategy is unclear. A natural question is whether intervention is effective in reducing the eventual toll of an epidemic. Such a reduction is limited by the fact that in the absence of permanent and broad lifestyle changes, we must eventually reach at least the herd immunity threshold in which a majority of the population has been infected (and gained immunity). Interventions can lessen the amount of epidemiological overshoot, but even this effect is limited. For the 1918 flu pandemic, studies reveal only a very weak—and not statistically significant—correlation between interventions and eventual death toll.

Many refinements of the SIR model exist, and researchers are applying several more detailed mathematical models to the current crisis. But the broad strokes of this article hold true for any reasonable model. While we cannot completely avoid the far-ranging consequences of this viral outbreak, mathematical modeling will help us know what to expect and how to prepare for and handle it.

The figures in this article were provided by the author.

References

- [1] Hatchett, R.J., Mecher, C.E., & Lipsitch, M. (2007). Public health interventions and epidemic intensity during the 1918 influenza pandemic. *Proc. Nat. Acad. Sci.*, 104(18), 7582-7587.
- [2] Hethcote, H.W. (2000). The mathematics of infectious diseases. *SIAM Rev.*, 42(4), 599-653.
- [3] Kermack, W.O., & McKendrick, A.G. (1927). A contribution to the mathematical theory of epidemics. *Proc. Roy. Soc. London. Series A, Containing papers of a mathematical and physical character*, 115(772), 700-721.

David I. Ketcheson is an associate professor of applied mathematics and computational science at King Abdullah University of Science and Technology (KAUST). He has written several blog posts about the mathematical modeling of COVID-19, which are available at <http://www.david-ketcheson.info/index.html>.

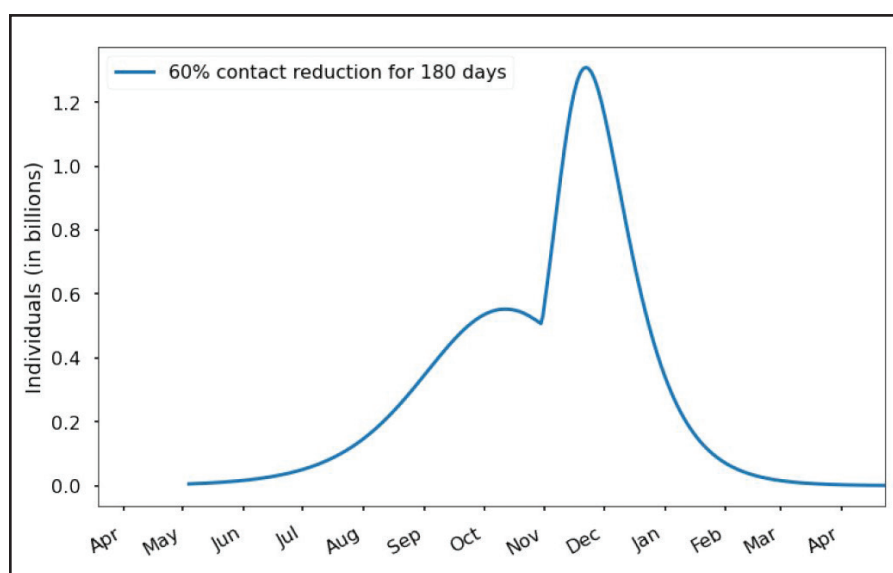
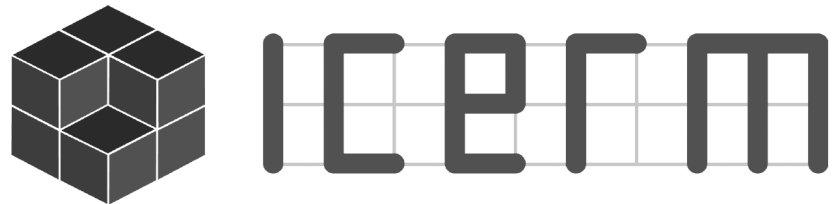


Figure 4. Scenario with a second outbreak after intervention is lifted.



Institute for Computational and Experimental Research in Mathematics

SEMESTER PROGRAM SPRING 2021

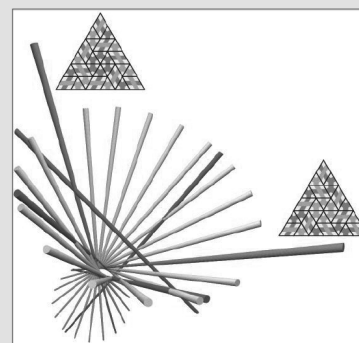
Combinatorial Algebraic Geometry

February 1 – May 7, 2021

Organizing Committee:

- Anders Buch**, Rutgers University
- Melody Chan**, Brown University
- June Huh**, Institute for Advanced Study and Princeton University
- Thomas Lam**, University of Michigan
- Leonardo Mihalcea**, Virginia Polytechnic Institute and State University
- Sam Payne**, University of Texas at Austin
- Lauren Williams**, Harvard University

Program Description:



Combinatorial algebraic geometry comprises the parts of algebraic geometry where basic geometric phenomena can be described with combinatorial data, and where combinatorial methods are essential for further progress.

Research in combinatorial algebraic geometry utilizes combinatorial techniques to answer questions about geometry. It also uses geometric methods to provide powerful tools for studying combinatorial objects. Much research in this area relies on mathematical software to explore and enumerate combinatorial structures and compute geometric invariants. Writing the required programs is a considerable part of many research projects. The development of new mathematics software is therefore prioritized in the program.

This program will bring together experts in both pure and applied parts of mathematics as well as mathematical programmers, all working at the confluence of discrete mathematics and algebraic geometry, with the aim of creating an environment conducive to interdisciplinary collaboration.

To learn more about ICERM programs, organizers, program participants, to submit a proposal, or to submit an application, please visit our website:

<https://icerm.brown.edu>

Ways to participate:

- Propose a:*
- semester program
 - topical or Hot Topics workshop
 - summer undergrad program
 - small group research project
- Apply for a:*
- semester program or workshop
 - postdoctoral fellowship
- Become an:*
- academic or corporate sponsor

About ICERM: The Institute for Computational and Experimental Research in Mathematics is a National Science Foundation Mathematics Institute at Brown University in Providence, Rhode Island. Its mission is to broaden the relationship between mathematics and computation.



121 S. Main Street, 11th Floor
Providence, RI 02903
401-863-5030
info@icerm.brown.edu

Seven SIAM Members Elected as AAAS Fellows

In October 2019, the American Association for the Advancement of Science (AAAS) elected 443 of its members as AAAS Fellows. This designation reflects the Fellows' efforts to advance science and its applications to better serve society. The Fellows collectively span the AAAS's 24 different sections, and seven members of SIAM were honored as 2019 Fellows within the Section on Mathematics:

- David M. Bressoud, *Macalester College*
- Lisa J. Fauci, *Tulane University*
- John S. Lowengrub, *University of California, Irvine*
- Michael J. Miksis, *Northwestern University*
- Kavita Ramanan, *Brown University*
- Jinchao Xu, *Pennsylvania State University*
- Kevin Zumbrun, *Indiana University*

To be considered for the rank of Fellow, an AAAS member must be nominated by three previously elected Fellows, the steering group of an AAAS section, or the organization's chief executive officer. Nominees undergo a two-step review process.

All incoming Fellows were recognized at the 2020 AAAS Annual Meeting, which took place this February in Seattle, Wash. Several of the honorees in the Section on Mathematics shared their thoughts and reactions with *SIAM News*.

David M. Bressoud: "I am very honored to have been elected as an AAAS Fellow. I admire their work as advocates for science, particularly all that they do to advance science and mathematics education, and I have been especially impressed by their

leadership on issues of equity. I am proud to be part of this organization."

Lisa J. Fauci (current SIAM president): "I was so pleased and honored to be named an AAAS Fellow! The AAAS is an organization that unites all of science, advocates for responsible science policy worldwide, and promotes scientific integrity. In recognizing members of the SIAM community, it asserts that applied mathematics and scientific computation are central to the scientific endeavor."

Michael J. Miksis: "The AAAS's membership encompasses the whole scientific and engineering community. Receiving recognition there is both an honor and a reminder that applied mathematics is a central and important part of the scientific and engineering enterprise. Enhancing our interactions with this diverse community helps us identify how applied mathematics can make significant contributions to problems facing society today."

Kavita Ramanan: "I am deeply humbled by this honor. Given the interdisciplinary nature of some of my own research in probability, I particularly value an organization like the AAAS, which unites researchers from different disciplines. I enjoyed attending talks outside my field at the AAAS Annual Meeting, some of which triggered new mathematical research questions, and hope that the math talks were of similar value to scientists. This recognition is even more special given that the broader goals of the AAAS—notably science advocacy and communication, international cooperation, and equity—align closely with my own."



Steven Chu, then-president of the American Association for the Advancement of Science (AAAS), inducts SIAM president Lisa Fauci (left) as a member of the 2019 class of AAAS Fellows during the 2020 AAAS Annual Meeting, which took place this February in Seattle, Wash. Photo courtesy of Robb Cohen Photography & Video.

Jinchao Xu: "Given the abundant resources in advanced computers and big data nowadays, mathematics is becoming increasingly important in science. As a computational mathematician, I am grateful for this recognition of my research, which provides bridges and tools that connect mathematical applications to different branches of science through analysis, modeling, data, and simulations. The AAAS offers an ideal platform to enhance interactions and collaborations between mathematicians and scientists in other fields."

Kevin Zumbrun: "I am deeply honored by the AAAS's recognition of my work. It is particularly meaningful to me that it comes from a society concerned with science across all fields, and one with which mathematics has traditionally not been so much associated. As mathematicians, we are all scientists; as applied mathematicians, exchange with other sciences is both goal and inspiration. Representation in the AAAS facilitates this exchange in both directions while simultaneously providing a voice in the larger exchange between science and society."

AI-based Repositioning

Continued from page 5

Nevertheless, the SARS-CoV main protease is relatively well-studied. Roughly 119 three-dimensional (3D) X-ray crystal structures of the SARS-CoV or SARS-CoV-2 main protease and its ligand complexes are in the Protein Data Bank (PDB),¹ and the binding affinities of more than 277 potential SARS main protease inhibitors are available in the ChEMBL database.² Additionally, there are 17,679 protein-ligand complexes—with binding affinities and 3D X-ray crystal structures—in the PDBbind 2019 general set. Moreover, the DrugBank³ contains about 1,600 drugs approved by the U.S. Food and Drug Administration (FDA), as well as nearly 6,000 experimental drugs. The aforementioned data provides a sound foundation for an SBDR machine learning model for SARS-CoV-2 main protease inhibition.

After selecting an appropriate target for COVID-19 drug repositioning, the next

challenge involves accurately screening existing drugs from the DrugBank. Over the last several decades, researchers have developed a wide variety of methods for virtual screening. It turns out that mathematics-based artificial intelligence (AI) approaches were top winners in recent years in the D3R Grand Challenge,⁴ a worldwide competition series in computer-aided drug design that is funded by the National Institutes of Health [11, 13]. Essentially, although deep learning algorithms—such as convolutional neural networks (CNNs)—can automatically extract features from simple data (e.g., images), they do not work well for data with intricate internal structures. In the case of macromolecules with intrinsically complex structures and high ML dimensionalities, AI approaches must invoke descriptors or representations to simplify their structural complexity and reduce their dimensionality.

Mathematics is a natural choice for data presentation. For example, topology [6]—especially persistent homology [1, 3]—

offers the so-called topological simplification that represents complex protein-drug interactions in terms of low-dimensional topological invariants or Betti numbers. Such invariants can be translational, rotational, and scale invariant, which is a requirement of ML [10]. Differential geometry, particularly differentiable manifold, provides a sophisticated abstraction of high-dimensional data [10]. The interplay among differential geometry, differential topology, and algebraic topology yields a variety of geometric, spectral, and topological representations [2].

Discrete mathematics—such as geometric graph theory, algebraic graph theory, topological graph theory, and combinatorics—is a prominent apparatus for data representation [4, 5, 10]. The integration of multiscale, spectral, and topological data analysis promises some of the most powerful data representations [8, 14]. Figure 1 (on page 5) depicts the use of mathematical representations to (i) construct *math-poses* that recreate 3D structures of protein-ligand complexes and (ii) extract *math-features* that contain critical chemical and biological information [13]. We pair *math-poses* and *math-features* with CNN, generative network complex, and reinforcement learning algorithms for protein-ligand pose selection, binding affinity prediction, ranking, scoring, and screening [9, 13].

One can utilize *in vitro* cell culture tests to validate top-ranking existing drugs inferred from virtual screening. The toxicities of FDA-approved drugs are known, which means that researchers can then bypass many steps in conventional drug discovery. Controlled clinical trials can further test the confirmed effective drugs to study their antiviral efficacy, dose, and frequency.

References

- [1] Carlsson, G. Zomorodian, A., Collins, A., & Guibas, L.J. (2005). Persistence barcodes for shapes. *Int. J. Shape Model.*, 11(02), 149-187.
- [2] Chen, J., Zhao, R., Tong, Y., & Wei, G.-W. (2019). Evolutionary de Rham-Hodge method. Preprint, *arXiv:1912.12388*.
- [3] Edelsbrunner, H., Letscher, D., & Zomorodian, A. (2000). Topological persistence and simplification. In *Proceedings*

41st annual symposium on foundations of computer science (pp. 454-463). Redondo Beach, CA: IEEE Computer Society.

[4] Heitsch, C., & Poznanović, S. (2014). Combinatorial insights into RNA secondary structure. In *Discrete and topological models in molecular biology* (pp. 145-166). New York, NY: Springer.

[5] Jonoska, N., & Twarock, R. (2008). Blueprints for dodecahedral DNA cages. *J. Phys. A: Math. Theor.*, 41(30), 304043.

[6] Kaczynski, T., Mischaikow, K., & Mrozek, M. (2006). *Computational homology*. In *Applied mathematical sciences* (Vol. 157). New York, NY: Springer Science & Business Media.

[7] Li, J., Zheng, S., Chen, B., Butte, A.J., Swamidass, S.J., & Lu, Z. (2016). A survey of current trends in computational drug repositioning. *Brief. Bioinform.*, 17(1), 2-12.

[8] Meng, Z., & Xia, K. (2020). Persistent spectral based machine learning (PerSpect ML) for drug design. Preprint, *arXiv:2002.00582*.

[9] Nguyen, D.D., & Wei, G.-W. (2019). AGL-Score: Algebraic graph learning score for protein-ligand binding scoring, ranking, docking, and screening. *J. Chem. Info. Model.*, 59(7), 3291-3304.

[10] Nguyen, D.D., Cang, Z., & Wei, G.-W. (2020). A review of mathematical representations of biomolecular data. *Phys. Chem. Chem. Phys.*, 22(8), 4343-4367.

[11] Nguyen, D.D., Cang, Z., Wu, K., Wang, M., Cao, Y., & Wei, G.-W. (2019). Mathematical deep learning for pose and binding affinity prediction and ranking in D3R Grand Challenges. *J. Comp.-Aided Mol. Des.*, 33(1), 71-82.

[12] Nguyen, D.D., Gao, K., Chen, J., Wang, R., & Wei, G.-W. (2020). Potentially highly potent drugs for 2019-nCoV. Preprint, *bioRxiv*.

[13] Nguyen, D.D., Gao, K., Wang, M., & Wei, G.-W. (2019). MathDL: Mathematical deep learning for D3R Grand Challenge 4. *J. Comp.-Aided Mol. Des.*, 34, 131-147.

[14] Wang, R., Nguyen, D.D., & Wei, G.-W. (2019). Persistent spectral graph. Preprint, *arXiv:1912.04135*.

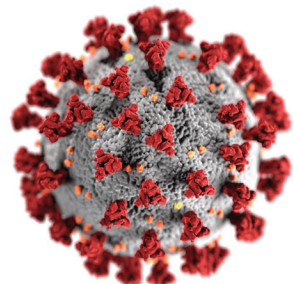
Duc D. Nguyen is an assistant professor of mathematics at Michigan State University. Guo-Wei Wei is a professor of mathematics at Michigan State University.

¹ <http://www wwpdb.org/>

² <https://www.ebi.ac.uk/chembl/>

³ <https://www.drugbank.ca/>

⁴ <https://drugdesigndata.org/about/grand-challenge>



The Power of 3D Printing in the Time of COVID-19

During the ongoing fight to combat COVID-19, the National Institutes of Health (NIH) has approved 3D-printed visors for personal protective equipment (PPE) face shields. The production of domestic face shields—which limit aerosol and droplet exposure—is racing to catch up with heightened demand. If you have a 3D printer, consider filling PPE supply gaps to help your local healthcare workers stay safe.

Printing and construction patterns are available at 3dprint.nih.gov/discover/3dpx-013359

Bowdoin College is one of many institutions that are using 3D printing to produce the NIH-approved visors.

Read more about the process at

bowdoin.edu/news/2020/04/bowdoin-produces-face-shields-for-medical-staff.html



SIAM Fellows

2020

SIAM is pleased to announce the newly selected Class of SIAM Fellows—a group of distinguished members of SIAM who were nominated by their peers for exceptional contributions to the fields of applied mathematics and computational science. Please join us in congratulating these 28 members of our community.



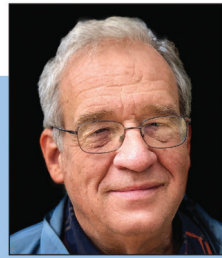
Srinivas Aluru
Georgia Institute of Technology



Steven Ashby
Pacific Northwest National Laboratory



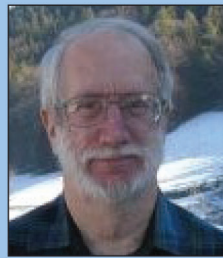
John P. Boyd
University of Michigan



Richard H. Byrd
University of Colorado Boulder



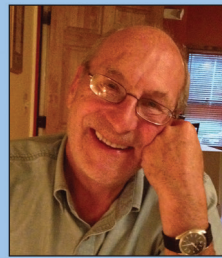
Ümit V. Çatalyürek
Georgia Institute of Technology



David Colton
University of Delaware



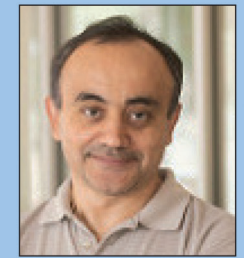
Jorge Cortes
University of California San Diego



George Cybenko
Dartmouth College



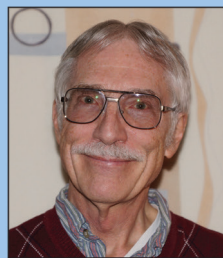
Alicia Dickenstein
Universidad de Buenos Aires and CONICET



Yalchin Efendiev
Texas A&M University



Martin J. Gander
Université de Genève



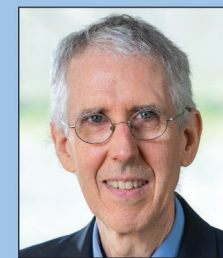
David M. Gay
AMPL Optimization, Inc



Laura Grigori
Inria



George Haller
ETH Zürich



Alfred Hero
University of Michigan



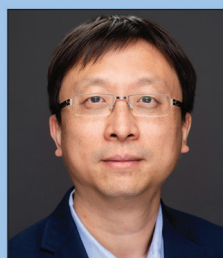
Kristin E. Lauter
Microsoft Research



Knut-Andreas Lie
SINTEF



Robert Lipton
Louisiana State University



Yi Ma
University of California, Berkeley



Kavita Ramanan
Brown University



Olaf Schenk
Università della Svizzera italiana



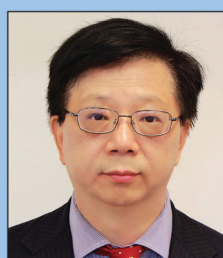
Jie Shen
Purdue University



Ronnie Sircar
Princeton University



Aravind Srinivasan
University of Maryland College Park



Defeng Sun
Hong Kong Polytechnic University



Ruth J. Williams
University of California San Diego



Barbara Wohlmuth
Technische Universität München



Pingwen Zhang
Peking University

Learn more about the 2020 Class of SIAM Fellows and nominate a colleague by October 21, 2020 for the 2021 Class of Fellows:

www.siam.org/Prizes-Recognition/Fellows-Program

A Model to Predict COVID-19 Epidemics with Applications to South Korea, Italy, and Spain

By Zhihua Liu, Pierre Magal,
Ousmane Seydi, and Glenn Webb

Our team has developed several differential equations models of COVID-19 epidemics [1-3] that use early reported case data from around the world to predict the future number of cases. These models incorporate three important elements of COVID-19: (1) the number of asymptomatic infectious individuals (with very mild or no symptoms), (2) the number of symptomatic reported infectious individuals (with severe symptoms), and (3) the number of symptomatic unreported infectious individuals (with less severe symptoms). They also decompose COVID-19 epidemics into three phases:

- Phase I, during which the number of cumulative reported cases increases linearly each day

- Phase II, during which the number of cumulative reported cases increases exponentially each day

- Phase III, during which the number of daily reported cases decreases each day.

The transitions between phases are generally difficult to determine, but one can estimate them from reported cases data as time progresses.

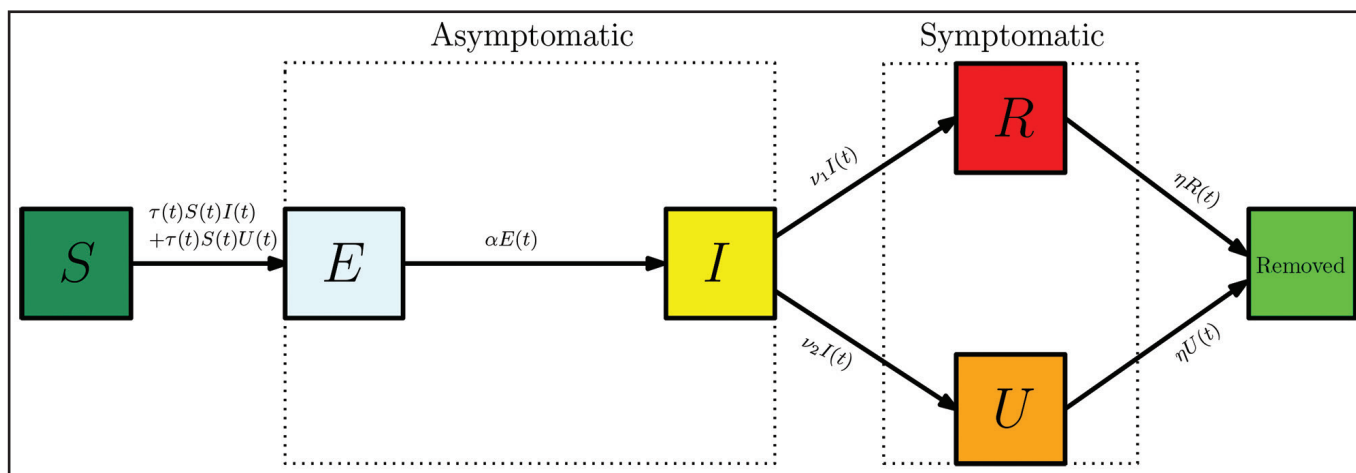


Figure 1. Compartments and flow chart of the model.

Our model consists of the following differential equations and initial conditions:

$$\begin{cases} S'(t) = -\tau(t)S(t)[I(t) + U(t)], \\ S(t_0) = S_0, \\ E'(t) = \tau(t)S(t)[I(t) + U(t)] - \alpha E(t), \\ E(t_0) = E_0, \\ I'(t) = \alpha E(t) - \nu I(t), \quad I(t_0) = I_0, \\ R'(t) = \nu_1 I(t) - \eta R(t), \quad R(t_0) = R_0, \\ U'(t) = \nu_2 I(t) - \eta U(t), \quad U(t_0) = U_0. \end{cases} \quad (1)$$

Here, $t \geq t_0$ is time in days, t_0 is the beginning date of the epidemic, $S(t)$ is the number of individuals susceptible to infection at time t , $E(t)$ is the number of asymptomatic noninfectious (exposed or latent infected) individuals at time t , $I(t)$ is the number of asymptomatic but infectious individuals at time t , $R(t)$ is the number of reported symptomatic infectious individuals at time t , and $U(t)$ is the number of unreported symptomatic infectious individuals at time t .

The time-dependent transmission rate parameter is $\tau(t)$. Newly-infected noninfectious asymptomatic individuals $E(t)$ incubate for an average period of $1/\alpha$ days. Asymptomatic infectious individuals $I(t)$ are infectious for an average period of $1/\nu$ days. Reported symptomatic infectious individuals $R(t)$ are infectious for an average period of $1/\eta$ days, as are unreported symptomatic infectious individuals $U(t)$. We assume that reported symptomatic infectious individuals $R(t)$ are reported and isolated immediately, and cause no further infections. One can also view the asymptomatic individuals $I(t)$ as having a low-level symptomatic state. All infections are acquired from either $I(t)$ or $U(t)$ infectious individuals. The fraction f of asymptomatic infec-

Country	χ_1	χ_2	t_0	t_1	μ	N	S_0	f	τ_0	\mathcal{R}_0
South Korea	0.758	0.287	Feb. 1	Feb. 22	0.6	Feb 27	51,700,000	0.8	1.05×10^{-8}	4.01
Italy	63.7	0.135	Feb. 10	Mar. 12	0.095	Mar. 16	60,500,000	0.4	4.16×10^{-9}	2.57
Spain	433.3	0.194	Feb. 3	Mar. 13	0.125	Mar. 20	46,700,000	0.4	7.11×10^{-9}	3.39

Figure 2. We obtain the parameters χ_1, χ_2 by fitting $\chi_1 \exp(\chi_2 t) - 1.0$ to the cumulative reported cases data between the dates $[t_1, t_2]$ for each country: (1) t_1 =February 22 to t_2 =March 1 for South Korea, (2) t_1 =March 12 to t_2 =March 21 for Italy, and (3) t_1 =March 13 to t_2 =March 21 for Spain. The values I_0, U_0, τ_0, t_0 , and \mathcal{R}_0 are obtained via equations (3)-(6). The parameters $\nu=1/6$, $\eta=1/7$, $\alpha=1/1$, $\chi_3=1.0$, and $R_0=1.0$ for all three countries.

tious cases becomes reported symptomatic infectious, and the fraction $1-f$ becomes unreported symptomatic infectious. The rate at which asymptomatic infectious cases become reported symptomatic is $\nu_1=f\nu$, and the rate at which asymptomatic infectious cases become unreported symptomatic is $\nu_2=(1-f)\nu$, where $\nu_1+\nu_2=\nu$.

The cumulative number of reported cases $CR(t)$ at time t is

$$CR(t) = \nu_1 \int_{t_0}^t I(\sigma) d\sigma, \quad t \geq t_0,$$

the cumulative number of unreported cases $CU(t)$ at time t is

$$CU(t) = \nu_2 \int_{t_0}^t I(s) ds, \quad t \geq t_0,$$

A COVID-19 epidemic transitions from phase I to phase II at time $t_1 > t_0$. Before t_1 , the cumulative number of reported cases increases linearly each day. After t_1 , the cumulative number of reported cases increases exponentially each day. We estimate the value of t_1 from data pertaining to the cumulative reported cases. We then fit an exponentially growing curve $CR(t)$ to the cumulative reported cases data in an estimated time interval $[t_1, t_2]$, according to the following formula:

$$CR(t) = \chi_1 \exp(\chi_2 t) - \chi_3, \quad t_1 \leq t \leq t_2. \quad (2)$$

We typically set $\chi_3=1$ but allow for other values. The initial value S_0 corresponds to

and the basic reproductive number is given by

$$R_0 = \frac{(\chi_2 + \nu)(\chi_2 + \alpha)(\chi_2 + \eta)}{\nu \alpha (\chi_2 + \eta + \nu_2)} \left(1 + \frac{(1-f)\nu}{\eta} \right). \quad (6)$$

We derive these formulas for $I_0, E_0, U_0, t_0, \tau_0$, and \mathcal{R}_0 in [1]; their values connect the phase II reported cases data to the parameterisation and initialisation of our differential equations model.

During phase II of the epidemic, $\tau(t) \equiv \tau_0$ is constant. When strong governmental measures like isolation, quarantine, and public closings are implemented, phase III begins. The timing of the implementation of these measures—and their subsequent impact on disease transmission—is complex. We use an exponentially decreasing time-dependent transmission rate $\tau(t)$ in phase III to incorporate these effects. The formula for $\tau(t)$, which has phase III beginning on day N , is

$$\begin{cases} \tau(t) = \tau_0, & 0 \leq t \leq N, \\ \tau(t) = \tau_0 \exp(-\mu(t-N)), & N < t. \end{cases} \quad (7)$$

We choose the date N and intensity μ of the public measures so that the cumulative reported cases in the epidemic's numerical simulation align with the cumulative reported case data at an identified date after day N . In this way, we can project forward the epidemic's time path after the government-imposed public measures take effect.

Applications

We apply our model to the COVID-19 epidemics in South Korea,¹ Italy,² and Spain.³ Figure 2 provides the parameters for these three countries.

COVID-19 Epidemic in South Korea: We divide the epidemic in South Korea into four stages (see Figure 3):

- (1) Before February 22: Phase I.
- (2) February 22 to March 1: Phase II.
- (3) March 2 to March 8: Phase III. The South Korean government implemented extensive testing, isolation, contact tracing of confirmed cases, and quarantine policies

See COVID-19 Epidemics on page 12

¹ https://en.wikipedia.org/wiki/2020_coronavirus_outbreak_in_South_Korea

² https://en.wikipedia.org/wiki/2020_coronavirus_outbreak_in_Italy

³ https://en.wikipedia.org/wiki/2020_coronavirus_outbreak_in_Spain

and the daily number of reported cases $DR(t)$ at time t is

$$\begin{cases} DR'(t) = \nu_1 I(t) - DR(t), \\ t \geq t_0, \quad DR(t_0) = DR_0. \end{cases}$$

Figure 1 depicts a flow diagram of the model.

Parameters

The fraction f of total reported symptomatic infectious cases is unknown and varies from region to region. We assume that $\eta=1/7$, which means that the average period of infectiousness of both unreported and reported symptomatic infectious individuals is seven days. We also assume that $\nu=1/6$, which means that the average period of infectiousness of asymptomatic infectious individuals is six days. Finally, we assume that $\alpha=1$, which means that the average period of exposed individuals is one day. We can modify these values as further epidemiological information becomes available; as of early April, they were consistent with accepted values.

the population of the reported cases data's region. The other initial conditions are

$$\begin{cases} I_0 = \frac{\chi_2 \chi_3}{f(\nu_1 + \nu_2)}, \quad E_0 = \frac{\chi_2 + \nu}{\alpha} I_0, \\ U_0 = \frac{\nu_2}{\chi_2 + \eta} I_0. \end{cases} \quad (3)$$

Furthermore, the value of t_0 (when $R(t_0) = CR(t_0) = 0$) for starting time t_0 of the epidemic is given by

$$CR(t_0) = 0 \Leftrightarrow \chi_1 \exp(\chi_2 t_0) - \chi_3 = 0 \Rightarrow$$

$$t_0 = \frac{1}{\chi_2} (\ln(\chi_3) - \ln(\chi_1)). \quad (4)$$

Additionally,

$$\begin{cases} \tau_0 = \frac{(\chi_2 + \alpha)E_0}{S_0[I_0 + U_0]} \\ \frac{(\chi_2 + \nu)(\chi_2 + \alpha)(\chi_2 + \eta)}{\alpha S_0(\chi_2 + \eta + \nu_2)}, \end{cases} \quad (5)$$

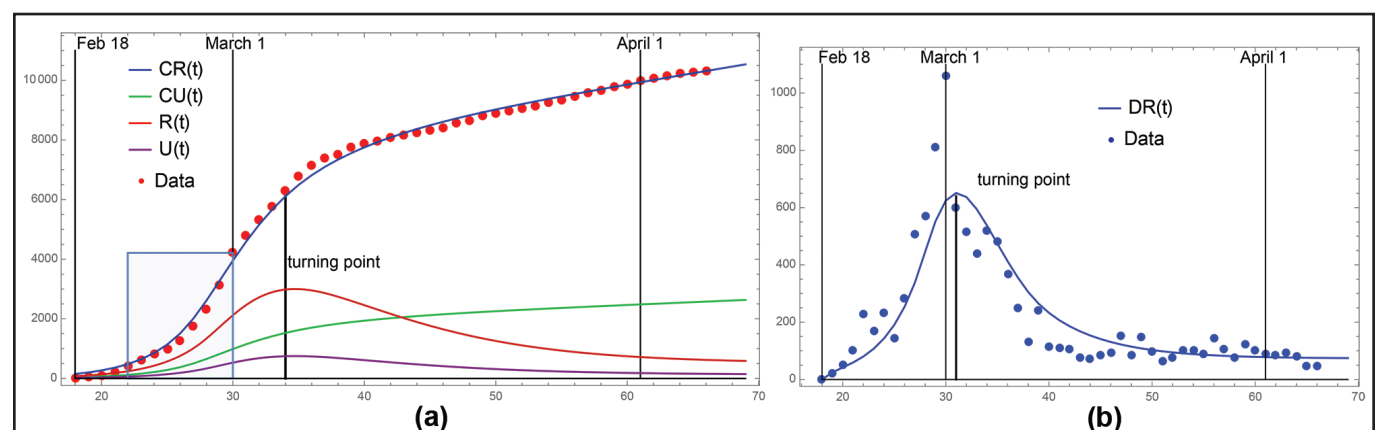


Figure 3. Model simulation for South Korea. **3a.** Cumulative reported cases. The shaded region = phase II and the model turning point is March 5. **3b.** Daily reported cases. The model turning point is March 5.

Lagrange Multiplier as Depth or Pressure

With bicycle season beginning in the Northeastern U.S., I would like to describe a small bike-related observation. It actually has nothing to do with a bicycle's mechanics; it simply occurred to me when I was riding my bike last fall. While climbing up a steep incline and observing a stream by the roadside, I asked myself the following question: *The water in any collection of connected vessels settles to the state of least potential energy; what is a mathematical expression of this obvious fact?* For cylindrical vessels it turned out to be the Cauchy-Schwarz inequality, as described in the November 2019 issue of *SIAM News*¹ (and in [2]). For polynomially tapered vessels, the expression yields Hölder's inequality [3].

These inequalities are therefore special cases of what every child knows: water levels equalize in communicating vessels. What other theorems are hiding behind this simple fact? In this month's column I provide one simple consequence; it would be interesting to discover more.

¹ <https://sinews.siam.org/Details-Page/the-cauchy-schwarz-inequality-and-a-paradoxpuzzle>

Incidentally, all of this—the Cauchy-Schwarz and Hölder inequalities, as well as the observation below—are, in the final analysis, *consequences of the law of conservation of energy*. Indeed, assume for a moment that water in communicating vessels settles at different levels. Then build a trough from the higher level to the lower one. The water will flow down this trough, and forever so due to the assumption, providing a free source of energy—a contradiction proving that the water settles at the same level, and also that this level minimizes potential energy.

As an aside, quite a few other geometrical theorems result from the impossibility of the perpetual motion machine [1].

Problem 1

Here is another problem that can be solved by the communicating vessels idea.

Given n functions $f_k: \mathbb{R}_+ \rightarrow \mathbb{R}_+$, $k=1, \dots, n$, minimize the sum

$$F(x_1, \dots, x_n) = \sum_{k=1}^n \int_0^{x_k} x f_k(x) dx, \quad (1)$$

subject to the constraint

$$G(x_1, \dots, x_n) = \sum_{k=1}^n \int_0^{x_k} f_k(x) dx = 1. \quad (2)$$

To interpret this problem² physically, imagine n vessels (as in Figure 1) with valves closed and the k th vessel filled with water of depth x_k . The sum (1) is thus the system's total potential energy (we choose the units in which the water density and gravitational accelerations are one unit). And (2) prescribes the total volume of water. Now as we open the valves in Figure 1, the potential energy F settles to its least value, which also corresponds to equal levels:

$$x_k = x_l \quad 1 \leq k, l \leq n. \quad (3)$$

The total volume G remains unchanged during the redistribution. This solves the problem: the minimizer is given by (3) and (2).

To verify the answer, the Lagrange multipliers method $\nabla F = \lambda \nabla G$ yields

$$x_k f(x_k) = \lambda f(x_k),$$

so that $x_k = \lambda$ for all $k=1, \dots, n$. As we already know, the levels of water equalize. But we now discover that *the Lagrange multiplier λ is the common water level, or equivalently, the water pressure at the bottom of the vessels*.

² To be more precise, we must assume that f_k are such that the constraint (2) is even satisfiable. I also probably should have said in fine print that $f_k \in L^1$, but I'll leave out these distracting details.

As a side remark, this problem generates the aforementioned inequalities for special choices of f_k .

Problem 2 (A Generalization)

Let $p_k: \mathbb{R}_+ \rightarrow \mathbb{R}_+$, $1 \leq k \leq n$ be monotone increasing functions, and let f_k be as it was before. Minimize

$$F_1(\mathbf{x}) = \sum_{k=1}^n \int_0^{x_k} p_k(x) f_k(x) dx,$$

subject to the same previous constraint (2). The Lagrange multiplier method $\nabla F_1 = \lambda \nabla G$ produces

$$p_k(x_k) = \lambda.$$

I leave it as a puzzle to build a thought-experimental “analog computer” that results in this answer and gives a physical interpretation of λ .

References

- [1] Levi, M. (2009). *The mathematical mechanic: Using physical reasoning to solve problems*. Princeton, NJ: Princeton University Press.
- [2] Levi, M. (2020). A water-based proof of the Cauchy-Schwarz Inequality. *Am. Math. Month.*, in press.
- [3] Levi, M., & Tokieda, T. (2020). A communicating-vessels proof of Hölder's inequality. *Am. Math. Month.*, in press.

Mark Levi (levi@math.psu.edu) is a professor of mathematics at the Pennsylvania State University.

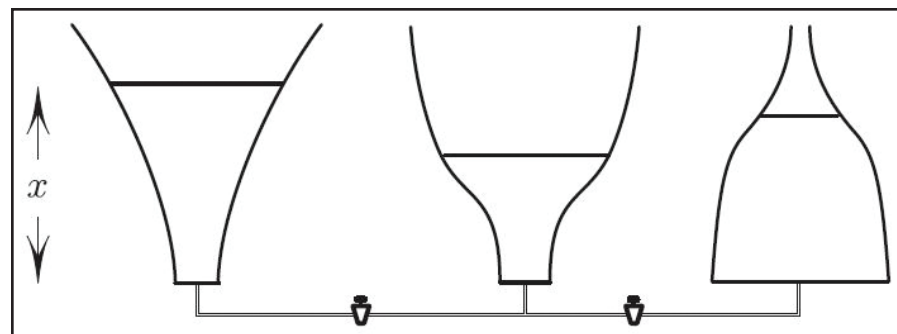



Figure 1. $f_k(x)$ is the area of the horizontal cross-section at height x of the k th vessel. Figure courtesy of Mark Levi.

SIAM Epidemiology Collection

In response to the ongoing COVID-19 pandemic, SIAM has opened a collection of 150+ epidemiology-related SIAM journal articles, proceedings, and book chapters. These materials will be freely available for one year. We hope that this content on epidemiology, infectious disease modeling, pandemics, and vaccines will contribute to the rapid fight against this global crisis.

To access the collection, please visit epubs.siam.org/page/EpidemiologyCollection



siam | Society for Industrial and Applied Mathematics
siam.org



WANTED: Book Reviewers

Have you recently come across an interesting book in the field of applied mathematics or computational science? Is there a book that you've been meaning to read that would appeal to the SIAM community? If so, would you like to review it for *SIAM News* readers?

Please send a pitch to sinews@siam.org with “Book review suggestion” in the subject line. *SIAM News* welcomes reviews of books with broad appeal in all areas served by SIAM.

SIAM can arrange for reviewers to receive free review copies. To be considered for review, a book's publication date should fall within the last year prior to review submission.



| Society for Industrial and Applied Mathematics
siam.org

Budget and Appropriations Outlook for FY 2021

By Ben Kallen

On February 10, 2020, President Trump released his fourth budget proposal to Congress. The fiscal year (FY) 2021 budget request reflects the political priorities of the Trump administration and kicks off the congressional appropriations process.

As with prior years, the request proposes drastic cuts to many of the non-defense federal agencies of interest to SIAM; increases to defense spending remain the administration's top priority. Consistent with the two-year budget agreement that was signed into law last year, the budget proposes spending \$740.5 billion on defense — a \$2.5 billion increase over the enacted level of FY 2020. In contrast, non-defense programs would be funded at \$590 billion, which is a cut of seven percent below current spending and far beneath the FY 2021 cap of \$634.5 billion that Congress established in last year's budget deal.

While Congress will decide final funding levels for FY 2021 and likely reject many

proposed cuts, the budget request still provides a useful window into major administration priorities, some of which have bipartisan support. For example, there is broad bipartisan support for increased investments in science and technology, especially in "Industries of the Future"—such as artificial intelligence (AI) and quantum information science—to maintain U.S. leadership and competitiveness.

The subsequent details describe how SIAM's priority agencies would fare under the aforementioned request:

- The National Science Foundation (NSF) would be funded at \$7.74 billion in FY 2021, a 6.5 percent or \$537 million cut below the FY 2020 enacted level. Within the NSF, the Division of Mathematical Sciences (DMS) would experience a reduction of 9.4 percent below the FY 2019 level for a total of \$214.8 million. The DMS is the source of more than 60 percent of all federal funding for mathematical research (FY 2020 funding figures for NSF directorates and divisions are not yet available).

- The Department of Energy's Office of Advanced Scientific Computing Research (ASCR) would be funded at \$988.1 million in FY 2021, which is a 0.8 percent or \$8.1 million increase from the FY 2020 enacted level. The Mathematical, Computational, and Computer Sciences Research account of the ASCR would receive \$264 million, an increase of 70 percent or \$109 million above FY 2020. This growth is driven by the ASCR's interest in shifting its agenda toward more future-focused research activities in emerging areas like AI/machine learning (ML) and quantum computing.

- The Department of Defense's basic research programs would be funded at \$2.32 billion in FY 2021, a 10.9 percent or \$284.2 million cut from the FY 2020 enacted level. The administration justifies these proposed reductions based on the need to reprioritize funding to support more substantial investments in national security priority areas such as AI/ML, hypersonics, microelectronics/5G, and space.

- The National Institutes of Health (NIH) would be funded at \$38.7 billion in FY 2021, a 7.2 percent or \$3 billion cut below the FY 2020 enacted level. Despite these planned reductions, the administration has proposed a new \$50 million initiative in the use of AI/ML to deepen understanding of the underpinnings of chronic diseases and identify promising treatments for these conditions. In the first year of this effort, the NIH would develop key AI and computational data resources, as well as new career pathways for recruiting and training investigators who work at the intersection of AI, data science, and biomedicine.

SIAM will continue to stay abreast of the FY 2021 appropriations cycle and its impact, advocate for strong funding for applied mathematics and computational science programs at relevant agencies, and keep members informed.

Ben Kallen is a government relations associate at Lewis-Burke Associates LLC.

COVID-19 Epidemics

Continued from page 10

after February 20. These measures took effect in daily reports after March 2.

(4) After March 8: The daily reported cases remained approximately the same each day, and the cumulative reported cases increased linearly. This stage corresponds to a new phase I, with a low-level background generation of reported cases each day.

To account for this new phase, we modify model (1) by replacing $\tau(t)$ with a novel transmission function $\tau(t, S(t), I(t), U(t))$ that depends on t , $S(t)$, $I(t)$, and $U(t)$ as follows:

$$\begin{cases} \tau(t, S(t), I(t), U(t)) = \tau_0, & t_0 \leq t \leq 27; \\ \tau(t, S(t), I(t), U(t)) = \tau_0 \exp(-0.6(t-27)), & 27 < t \leq 37; \\ \tau(t, S(t), I(t), U(t)) = 23.0\tau_0 \exp(-0.6(37-27)) \left(\frac{S(37)[I(37)+U(37)]}{S(t)[I(t)+U(t)]} \right), & 37 < t. \end{cases} \quad (8)$$

We select the value 23.0 to match the slope of the linear increasing cumulative reported cases data after day 37. The equations and initial values remain the same, with the exception of this novel τ function. The formulas in (8) connect the new phase I to the transmission rate in the model equations and the model outputs of $E(t)$, $I(t)$, $U(t)$, $R(t)$, $CU(t)$, $CR(t)$, and $DR(t)$. One can apply the form of (8) to other examples that transition from phase III to a new phase I, corresponding to a linearly-increasing growth rate of cumulative reported cases. This new phase I can further transform to yet another phase I with a slower linearly increasing growth rate.

COVID-19 Epidemic in Italy: We divide the epidemic in Italy into three stages (see Figure 4):

- (1) Before March 12: Phase I.
- (2) March 12 to March 21: Phase II.
- (3) After March 24: Phase III. Beginning on March 1, the Italian government implemented extensive public regional lockdown measures, which were extended to all of Italy on March 10. These measures started to reduce the number of reported daily cases approximately two weeks later.

COVID-19 Epidemic in Spain: We divide the epidemic in Spain into three stages (see Figure 5):

- (1) Before March 13: Phase I.
- (2) March 13 to March 21: Phase II.
- (3) After March 28: Phase III. The Spanish government implemented partial shutdown measures on March 13 and imposed a general state of alarm for all of Spain on March 14. These measures started to reduce the number of reported daily cases approximately two weeks later.

Concluding Thoughts

We have applied a new method [1-3] to predict a COVID-19 epidemic's evolution in a particular geographical region, based on reported cases data from that region. Our model focuses on unreported cases,

asymptomatic infectious cases, and division of the epidemic's evolution through a succession of phases. Our method can be predictive when the epidemic is growing exponentially in phase II. Specifically, we demonstrate a technique to identify the exponentially increasing rate of cumulative reported cases in phase II [3]. When public measures to ameliorate the epidemic begin during this phase, we model these measures with a time-dependent exponentially decreasing transmission rate. These mitigations result in phase III: a subsequent reduction in daily reported cases. We determine the transition from phase II to phase III—which may require more than a week—in the model simulations.

The epidemic has attenuated in South Korea because of major measures that encourage social distancing. These measures involve surveillance, extensive testing, and isolation and contact tracing for reported and suspected cases. However, the cumulative number of reported cases in South Korea has not flattened; instead, it is growing linearly at a low rate. The epidemics in Italy and Spain have evidently passed the turning point, according to data about the daily reported

cases. The cumulative reported cases may not flatten but instead continue to grow linearly at a low rate, as in South Korea.

Our model incorporates government and social distancing measures through the time-dependent transmission rate τ . These measures should begin as early as possible and be as strong as possible. If such efforts cause the epidemic to substantially subside, the situation in South Korea indicates that a background level of daily cases may persist for an extended time. If countries reduce major distancing measures too early or too extensively, the epidemic can enter a new phase II and undergo another exponential increase in cumulative cases. Control of COVID-19 epidemics is possible, as evidenced by the situation in South Korea. The future of COVID-19 and its human toll is currently uncertain, and we hope that mathematical models will be of use.

The figures in this article were provided by the authors.

References

- [1] Liu, Z., Magal, P., Seydi, O., & Webb, G. (2020). A COVID-19 epidemic model with latency period. To appear.
- [2] Liu, Z., Magal, P., Seydi, O., & Webb, G. (2020). Predicting the cumulative number of cases for the COVID-19 epidemic in China from early data. Preprint, *medRxiv*.
- [3] Liu, Z., Magal, P., Seydi, O., & Webb, G. (2020). Understanding unreported cases in the 2019-nCoV epidemic outbreak in Wuhan, China, and the importance of major public health interventions. *MPDI Biol.*, 9(3), 50.

Zhihua Liu is a professor in the School of Mathematical Sciences at Beijing Normal University in China. Pierre Magal is a professor of mathematics at the University of Bordeaux in France. Ousmane Seydi is an assistant professor at Ecole Polytechnique de Thiès in Senegal. Glenn Webb is a professor of mathematics at Vanderbilt University.

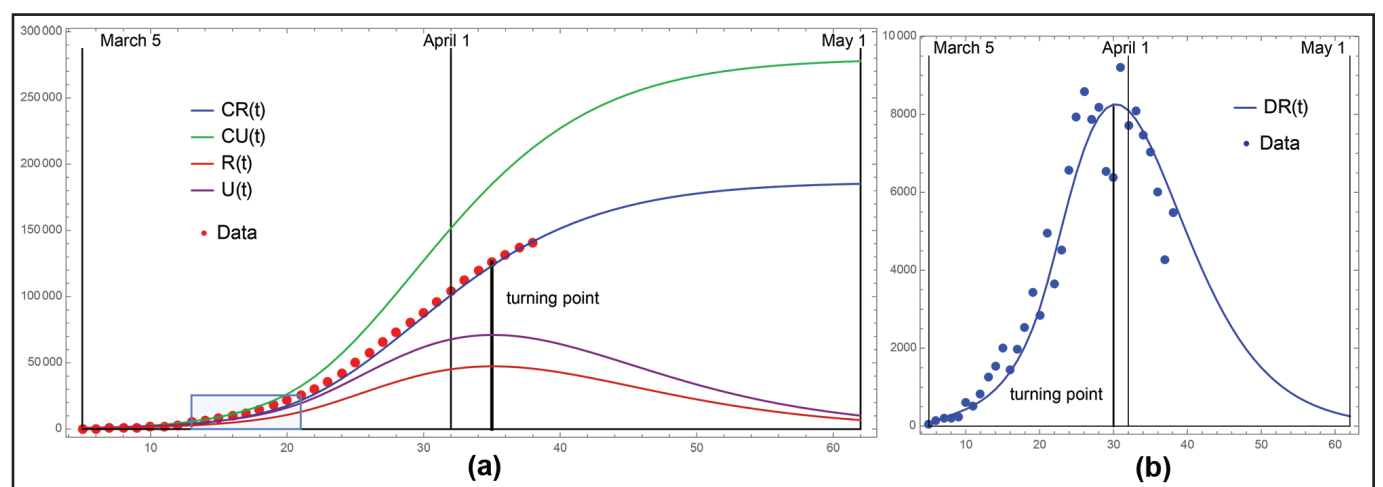


Figure 5. Model simulation for Spain. 5a. Cumulative reported cases. The shaded region = phase II and the model turning point is April 4. 5b. Daily reported cases. The model turning point is March 30.

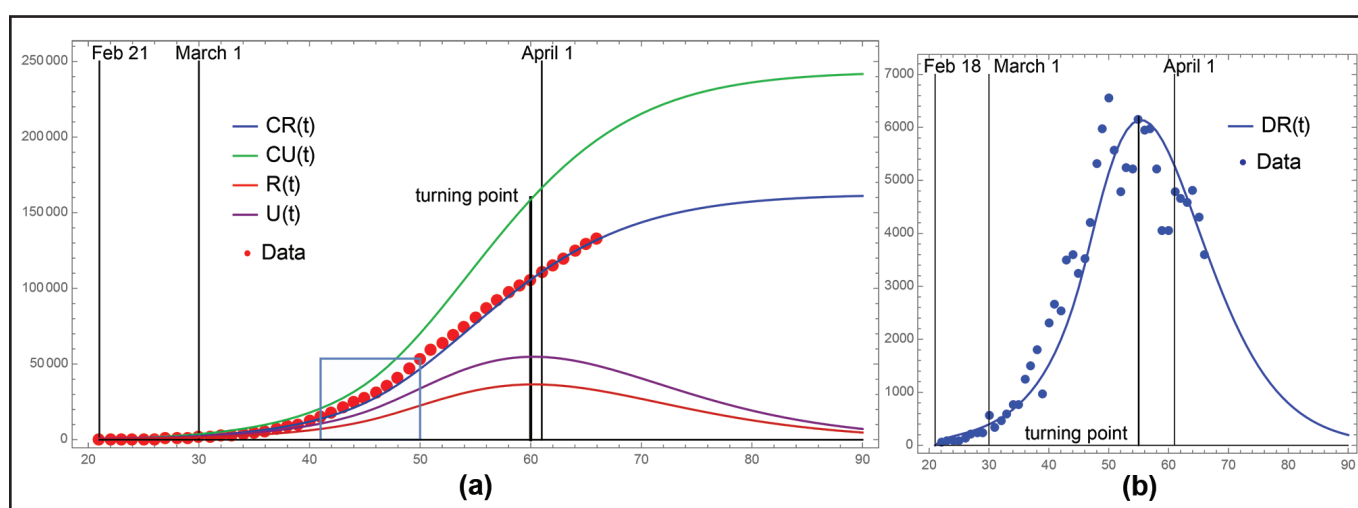


Figure 4. Model simulation for Italy. 4a. Cumulative reported cases. The shaded region = phase II and the model turning point is March 31. 4b. Daily reported cases. The model turning point is March 26.